

Supporting Information for

**Bifunctional silanol-based HBD catalysts for CO₂ fixation into cyclic
carbonates**

*Jovana Pérez-Pérez,^{a,b} Uvaldo Hernández-Balderas^{a,b} Diego Martínez-Otero,^{a,b}
and Vojtech Jancik^{a,b,*}*

^a Universidad Nacional Autónoma de México, Instituto de Química, Ciudad
Universitaria, Ciudad de México, 04510, México.

^b Centro Conjunto de Investigación en Química Sustentable UAEM-UNAM, Carr.
Toluca-Atlacomulco km 14.5, 50200 Toluca, Estado de México, México.

*vjancik@unam.mx (V. Jancik)

List of figures

Fig. S1 ^1H NMR spectrum of compound 2	4
Fig. S2 ^{13}C NMR spectrum of compound 2	5
Fig. S3 ^{29}Si NMR spectrum of compound 2	5
Fig. S4 ^1H NMR spectrum of compound 3	6
Fig. S5 ^{13}C NMR spectrum of compound 3	7
Fig. S6 ^{29}Si NMR spectrum of compound 3	7
Fig. S7 ^1H NMR spectrum of compound 4	8
Fig. S8 ^{13}C NMR spectrum of compound 4	9
Fig. S9 ^{29}Si NMR spectrum of compound 4	9
Fig. S10 ^1H NMR spectrum of compound 5	10
Fig. S11 ^{13}C NMR spectrum of compound 5	11
Fig. S12 ^{29}Si NMR spectrum of compound 5	11
Fig. S13 ^1H NMR spectrum of compound (<i>Rac</i>)- 6	12
Fig. S14 ^{13}C NMR spectrum of compound (<i>Rac</i>)- 6	13
Fig. S15 ^{29}Si NMR spectrum of compound (<i>Rac</i>)- 6	13
Fig. S16 ^1H NMR spectrum of compound (<i>R</i>)- 6	14
Fig. S17 ^{13}C NMR spectrum of compound (<i>R</i>)- 6	15
Fig. S18 ^{29}Si NMR spectrum of compound (<i>R</i>)- 6	15
Fig. S19 ^1H NMR spectrum of compound 7	16
Fig. S20 ^{13}C NMR spectrum of compound 7	17
Fig. S21 ^{29}Si NMR spectrum of compound 7	17
Fig. S22 ^1H NMR spectrum of compound 8	18
Fig. S23 ^{13}C NMR spectrum of compound 8	19
Fig. S24 ^{29}Si NMR spectrum of compound 8	19
Fig. S25 ^1H NMR spectrum of compound 9	20
Fig. S26 ^{13}C NMR spectrum of compound 9	21
Fig. S27 ^{29}Si NMR spectrum of compound 9	21
Fig. S28 ^1H NMR spectrum of compound 10	22
Fig. S29 ^{13}C NMR spectrum of compound 10	23
Fig. S30 ^{29}Si NMR spectrum of compound 10	23
Fig. S31 ^1H NMR spectrum of compound (<i>Rac</i>)- 11	24
Fig. S32 ^{13}C NMR spectrum of compound (<i>Rac</i>)- 11	25
Fig. S33 ^{29}Si NMR spectrum of compound (<i>Rac</i>)- 11	25
Fig. S34 ^1H NMR spectrum of compound (<i>R</i>)- 11	26
Fig. S35 ^{13}C NMR spectrum of compound (<i>R</i>)- 11	27
Fig. S36 ^{29}Si NMR spectrum of compound (<i>R</i>)- 11	27
Fig. S37 ^1H NMR spectrum of compound 12	28
Fig. S38 ^{13}C NMR spectrum of compound 12	29
Fig. S39 ^{29}Si NMR spectrum of compound 12	29
Fig. S40 ^1H NMR spectrum of compound (<i>Rac</i>)- 13	30
Fig. S41 ^{13}C NMR spectrum of compound (<i>Rac</i>)- 13	31
Fig. S42 ^{29}Si NMR spectrum of compound (<i>Rac</i>)- 13	31
Fig. S43 ^1H NMR spectrum of compound (<i>R</i>)- 13	32

Fig. S44 ^{13}C NMR spectrum of compound (<i>R</i>)- 13	33
Fig. S45 ^{29}Si NMR spectrum of compound (<i>R</i>)- 13	33
Fig. S46 ^1H NMR spectrum of styrene carbonate 15a	34
Fig. S47 ^1H NMR spectrum of (<i>Rac</i>)-1,2-butylene carbonate 15b	35
Fig. S48 ^1H NMR spectrum of (<i>R</i>)-1,2-butylene carbonate 15c	36
Fig. S49 ^1H NMR spectrum of 3-phenoxypropylene carbonate 15d	37
Fig. S50 ^1H NMR spectrum of 3-chloropropylene carbonate 15e	38
Fig. S51 ^1H NMR spectrum of 4-chlorostyrene carbonate 15f	39
Fig. S52 ^1H NMR spectrum of 4-fluorostyrene carbonate 15g	40
Fig. S53 ^1H NMR spectrum of cyclohexene carbonate 15h	41

List of tables

Table S1 Selected highly active catalysts for the cycloaddition of epoxides and CO_2	43
Table S2 Selected crystallographic data for compounds 12 , (<i>Rac</i>)- 13 and (<i>R</i>)- 13	44

¹H RMN (300 MHz, CDCl₃)

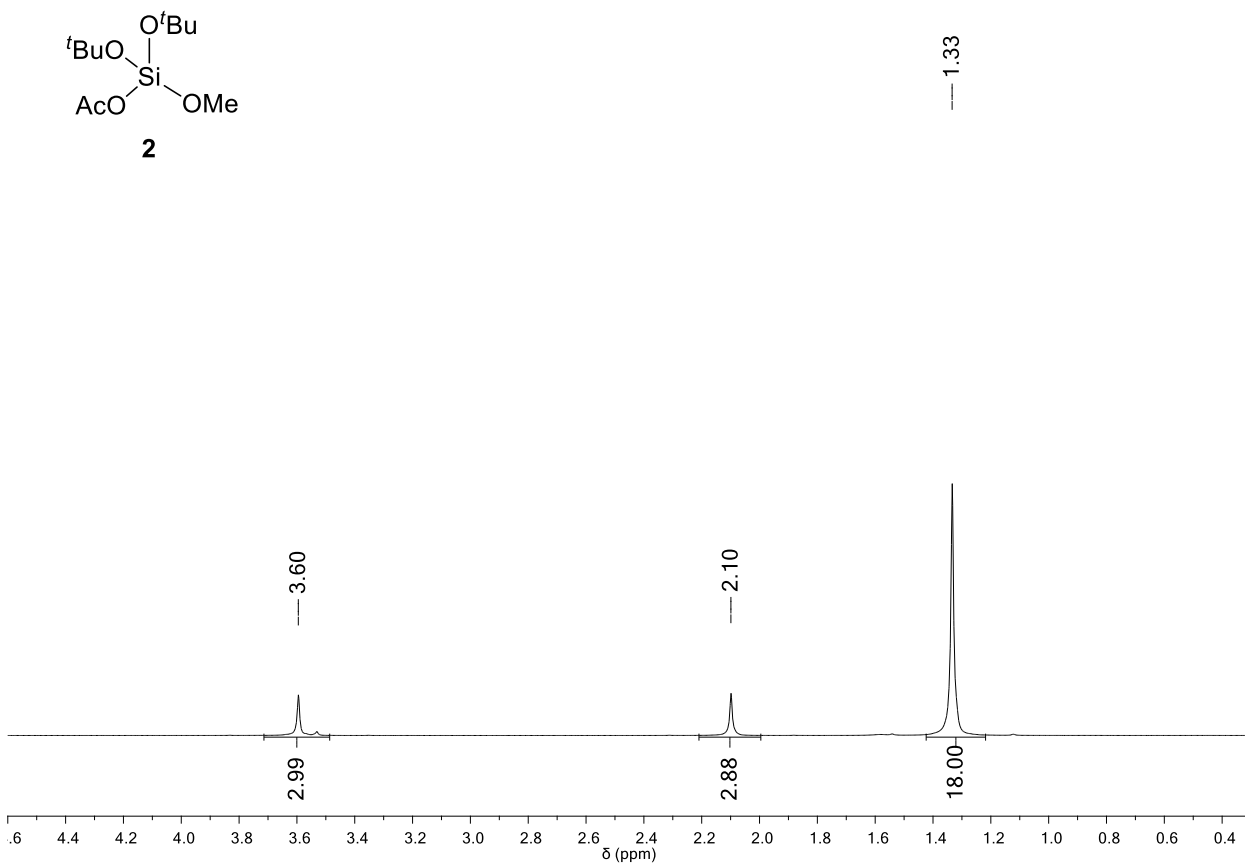


Fig. S1 ¹H NMR spectrum of compound **2**.

^{13}C RMN (75 MHz, CDCl_3)

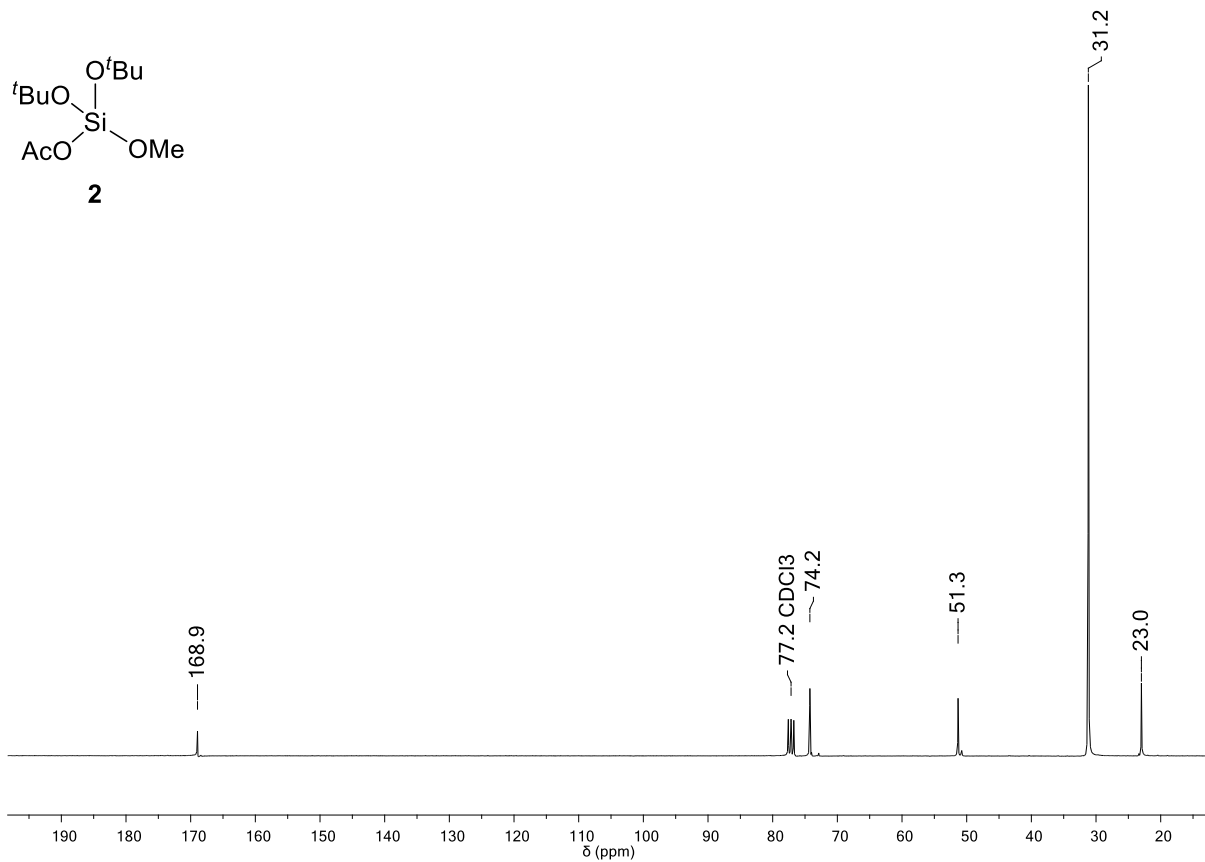


Fig. S2 ^{13}C NMR spectrum of compound **2**.

^{29}Si RMN (60 MHz, CDCl_3)

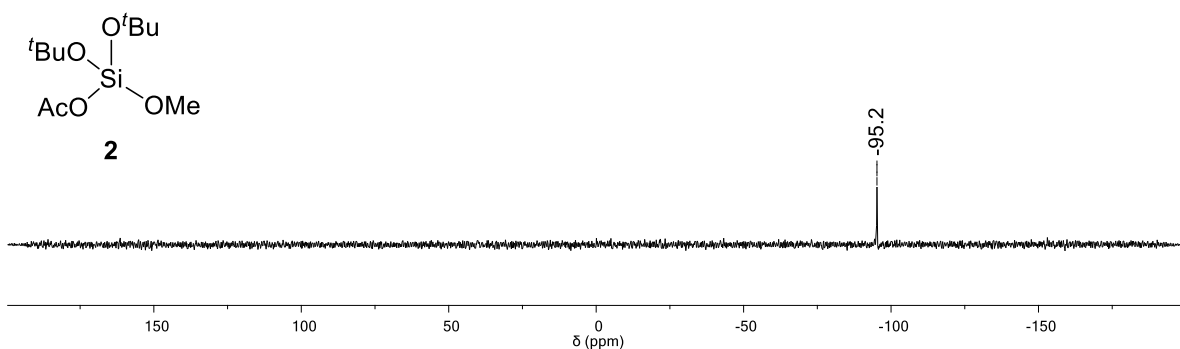


Fig. S3 ^{29}Si NMR spectrum of compound **2**.

^1H RMN (300 MHz, CDCl_3)

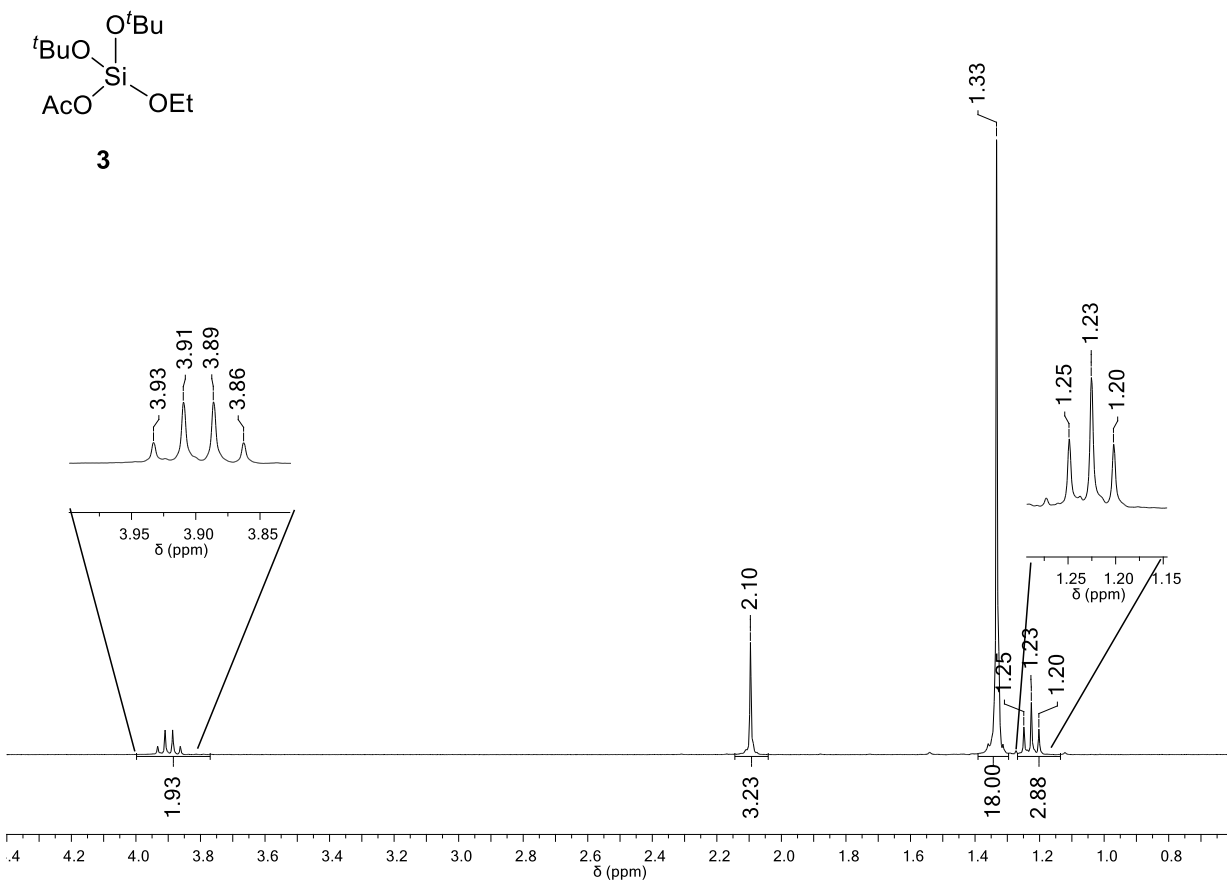


Fig. S4 ^1H NMR spectrum of compound **3**.

^{13}C RMN (75 MHz, CDCl_3)

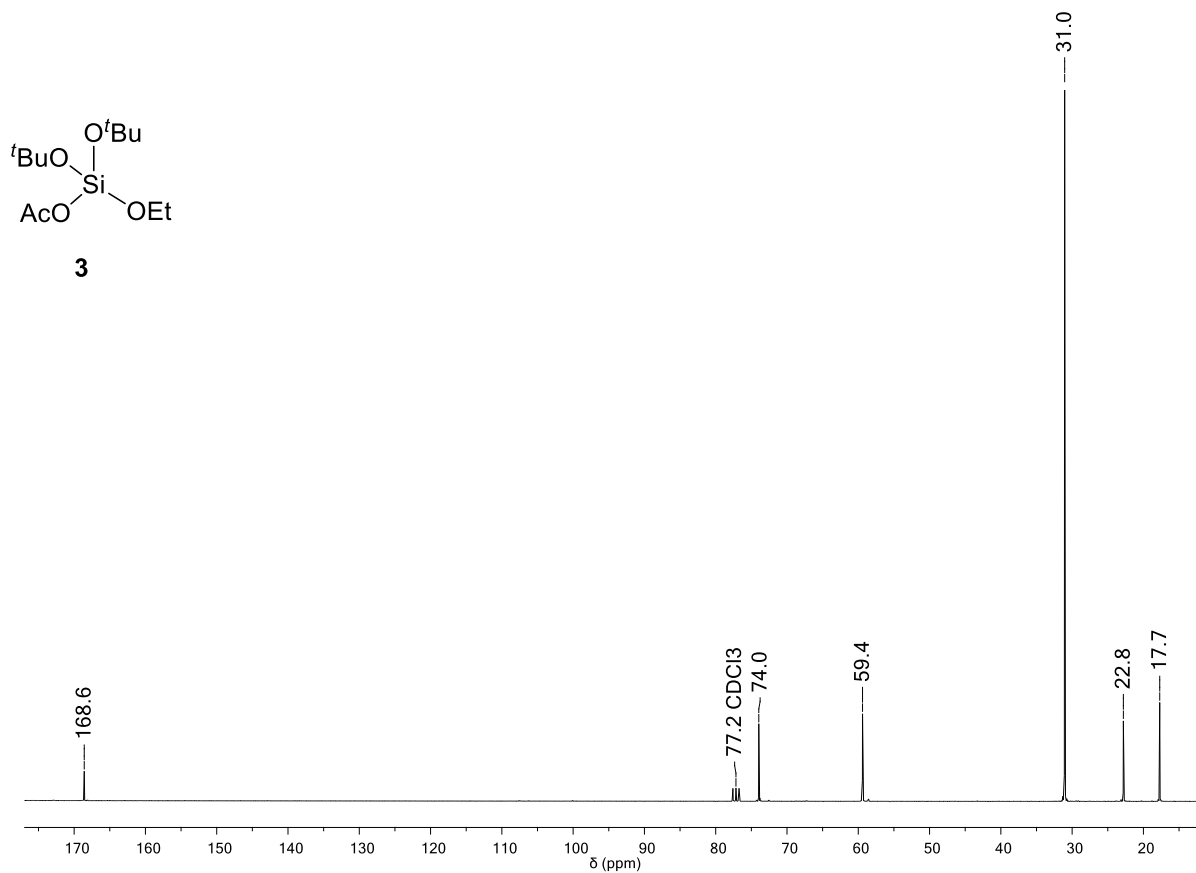


Fig. S5 ^{13}C NMR spectrum of compound 3.

^{29}Si RMN (60 MHz, CDCl_3)

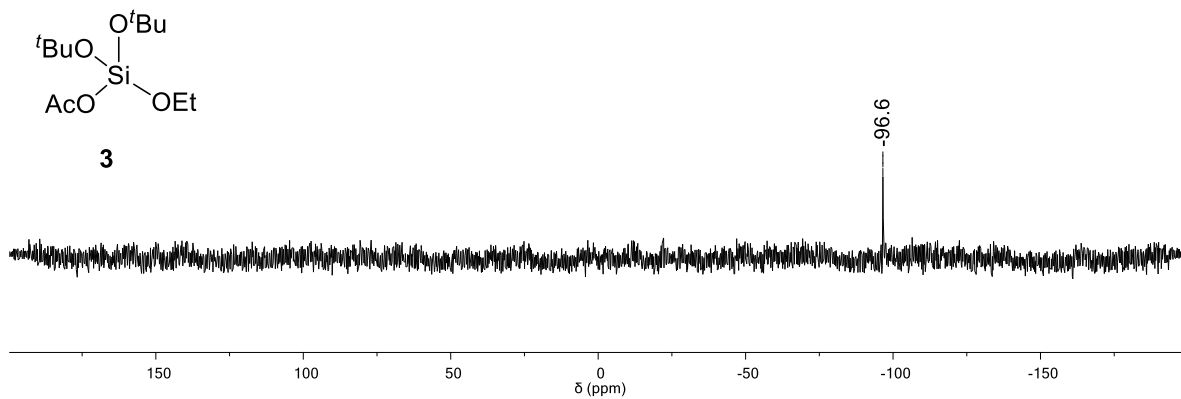
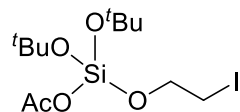


Fig. S6 ^{29}Si NMR spectrum of compound 3.

¹H RMN (300 MHz, CDCl₃)



4

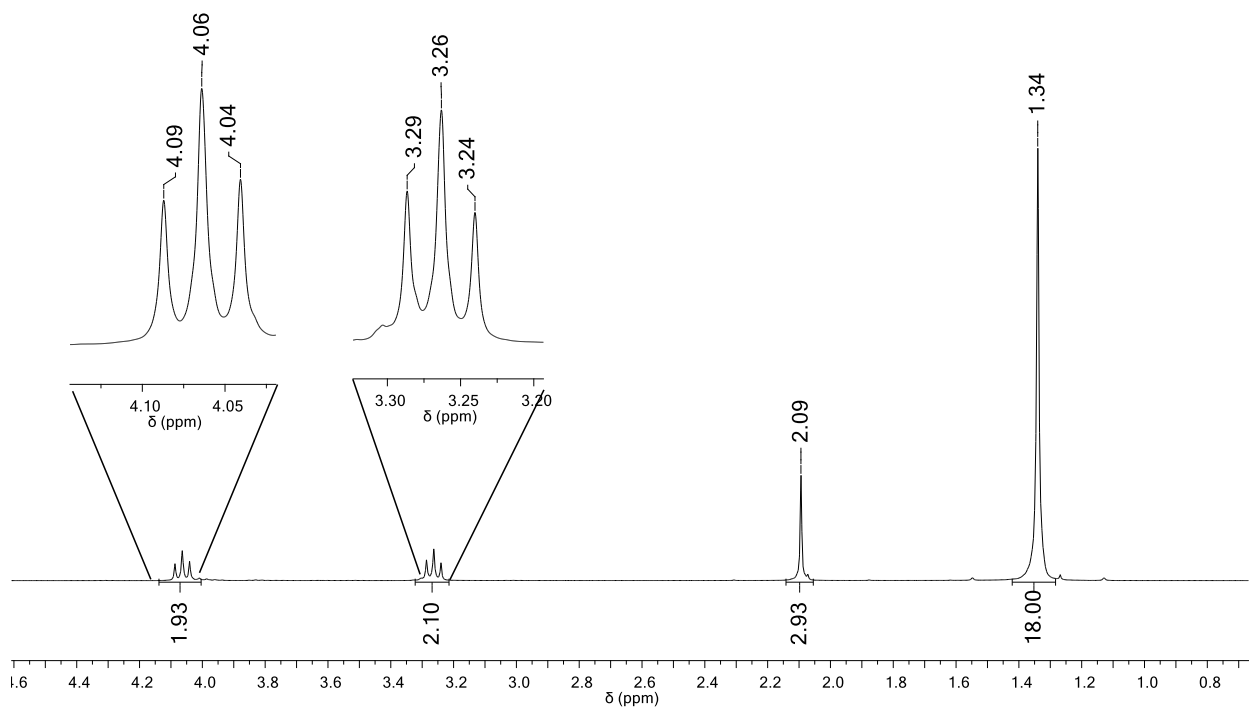


Fig. S7 ¹H NMR spectrum of compound 4.

^{13}C RMN (75 MHz, CDCl_3)

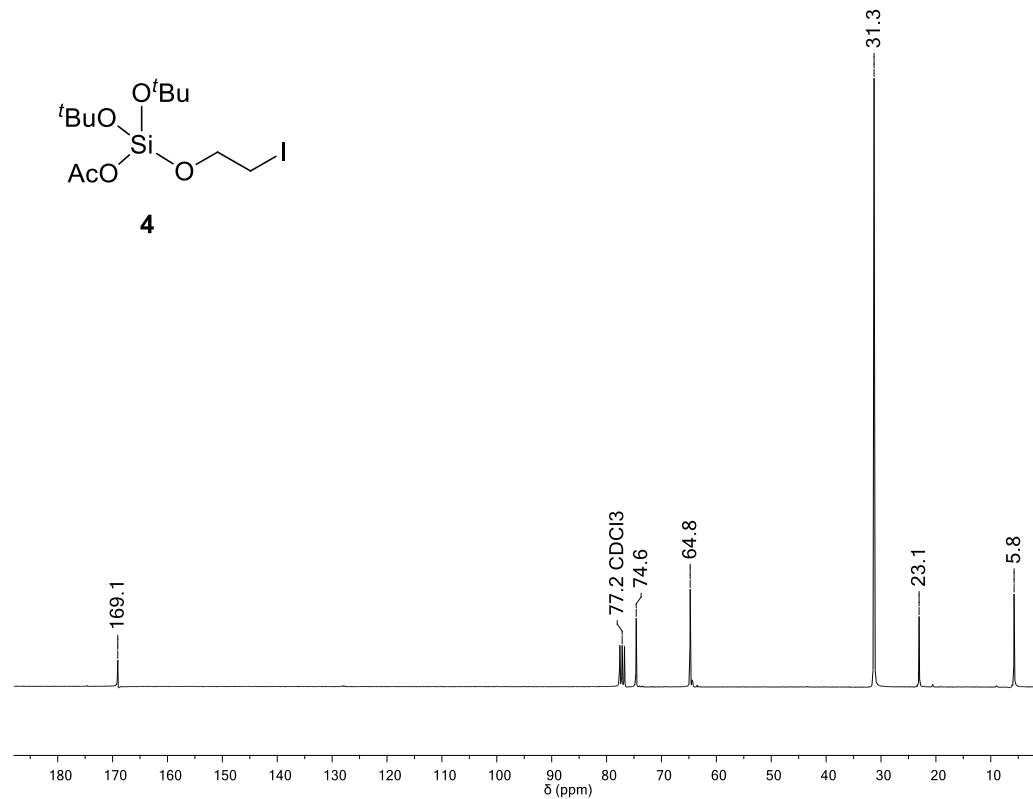


Fig. S8 ^{13}C NMR spectrum of compound 4.

^{29}Si RMN (60 MHz, CDCl_3)

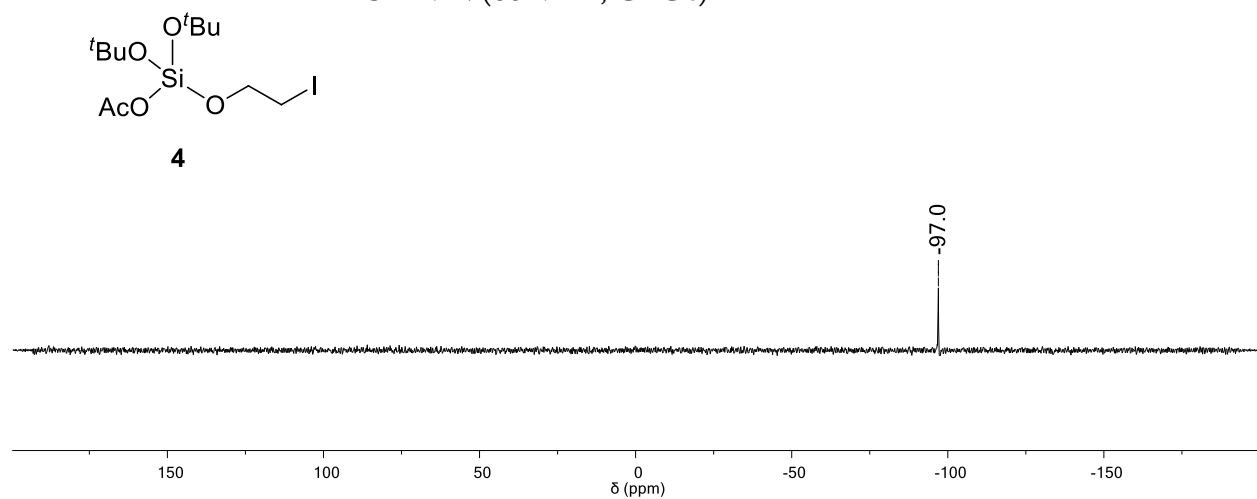


Fig. S9 ^{29}Si NMR spectrum of compound 4.

¹H RMN (300 MHz, CDCl₃)

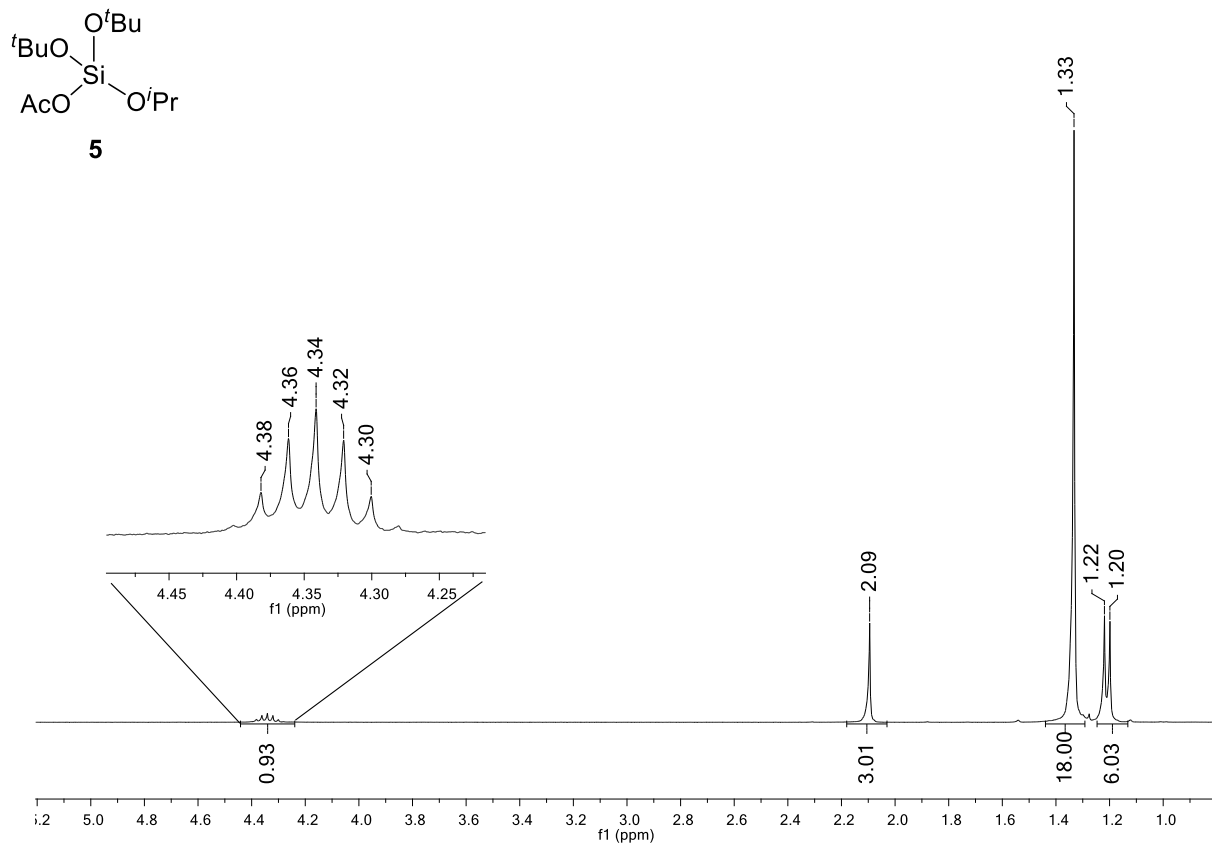


Fig. S10 ¹H NMR spectrum of compound **5**.

^{13}C RMN (75 MHz, CDCl_3)

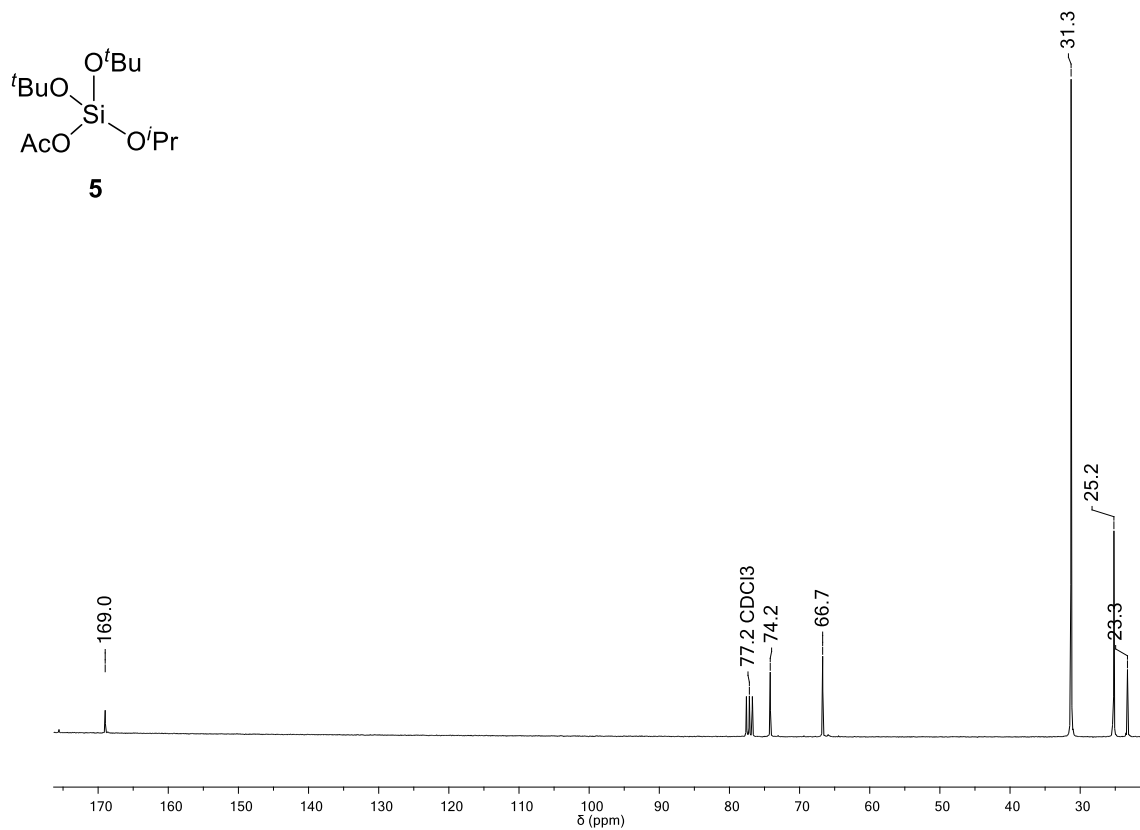


Fig. S11 ^{13}C NMR spectrum of compound **5**.

^{29}Si RMN (60 MHz, CDCl_3)

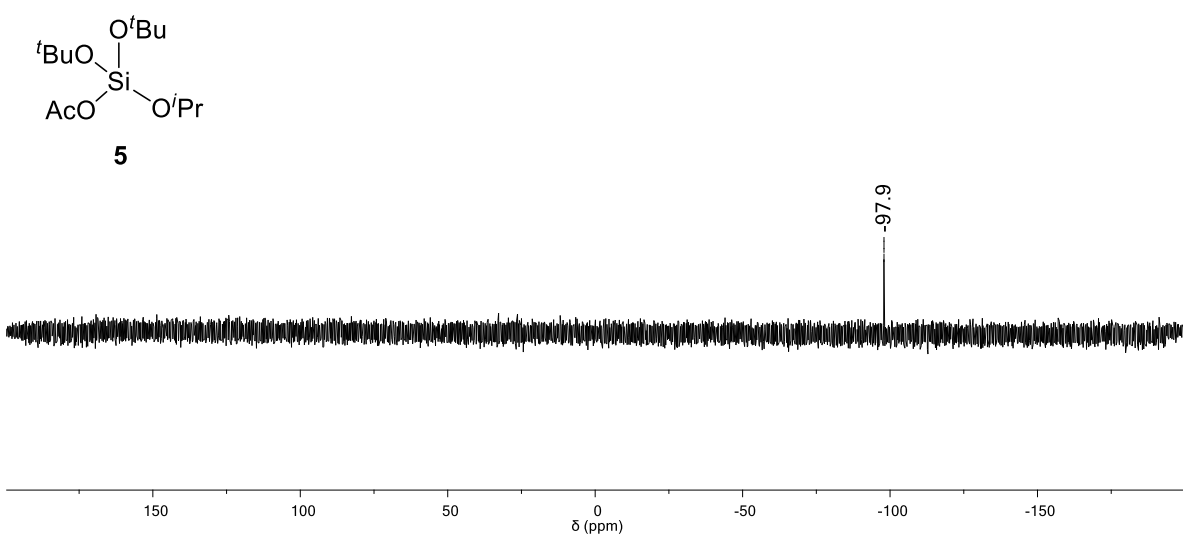


Fig. S12 ^{29}Si NMR spectrum of compound **5**.

¹H RMN (300 MHz, CDCl₃)

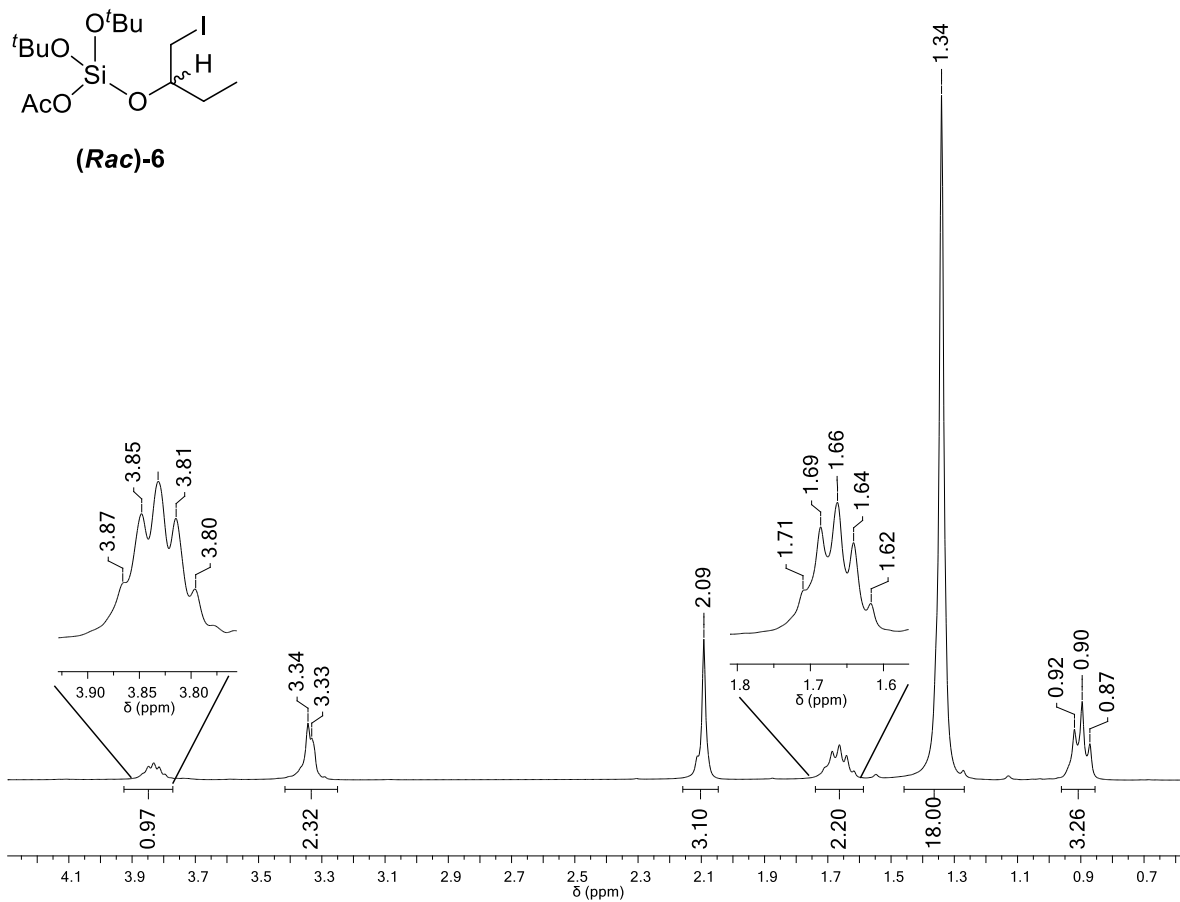


Fig. S13 ¹H NMR spectrum of compound (Rac)-6.

^{13}C RMN (75 MHz, CDCl_3)

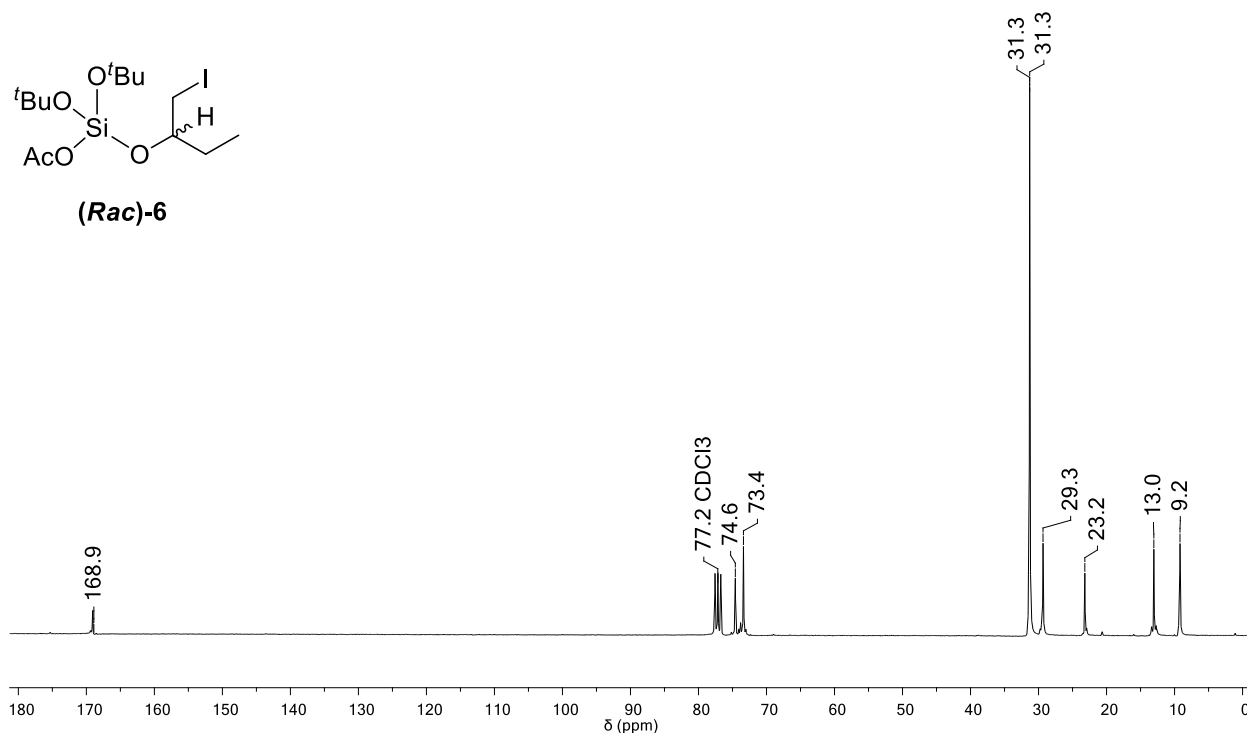


Fig. S14 ^{13}C NMR spectrum of compound (Rac)-6.

^{29}Si RMN (60 MHz, CDCl_3)

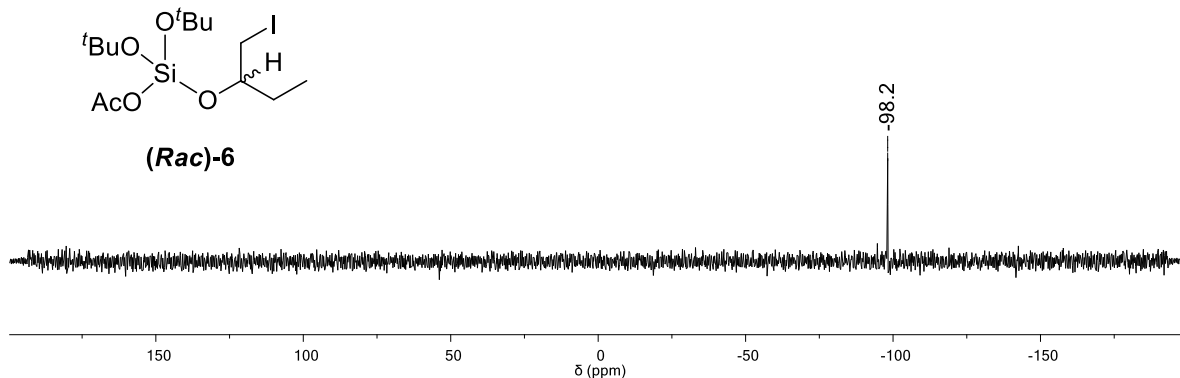


Fig. S15 ^{29}Si NMR spectrum of compound (Rac)-6.

¹H RMN (300 MHz, CDCl₃)

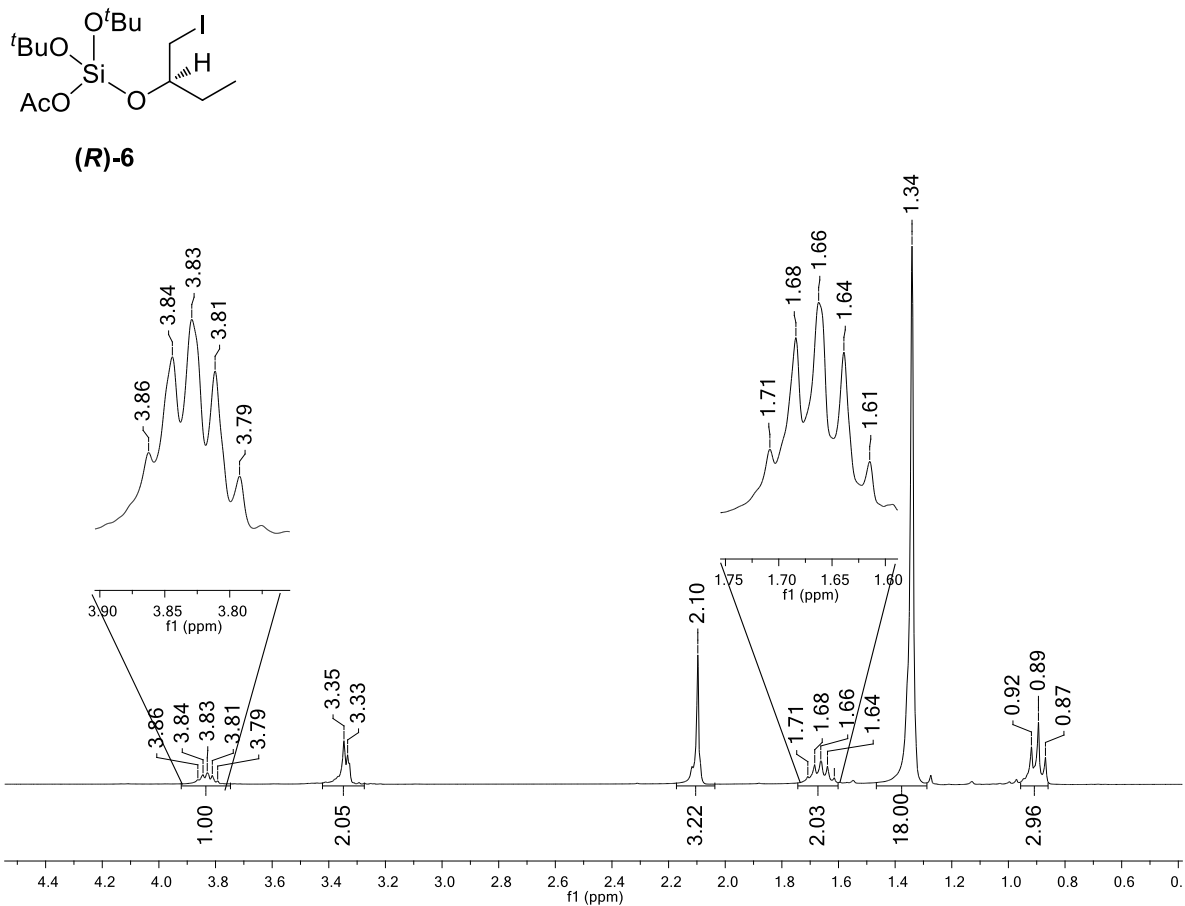


Fig. S16 ¹H NMR spectrum of compound (R)-6.

^{13}C RMN (75 MHz, CDCl_3)

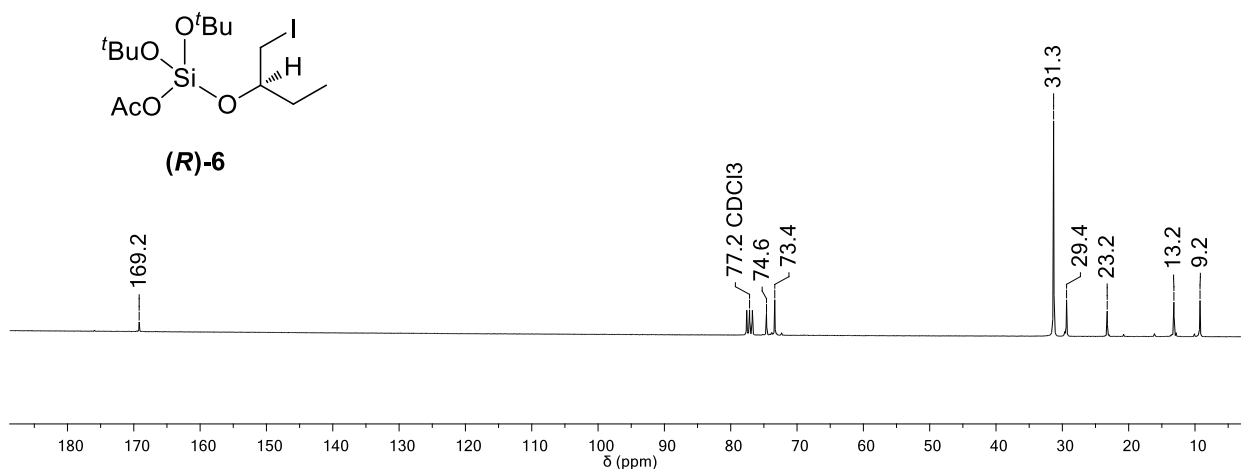


Fig. S17 ^{13}C NMR spectrum of compound (R) -6.

^{29}Si RMN (60 MHz, CDCl_3)

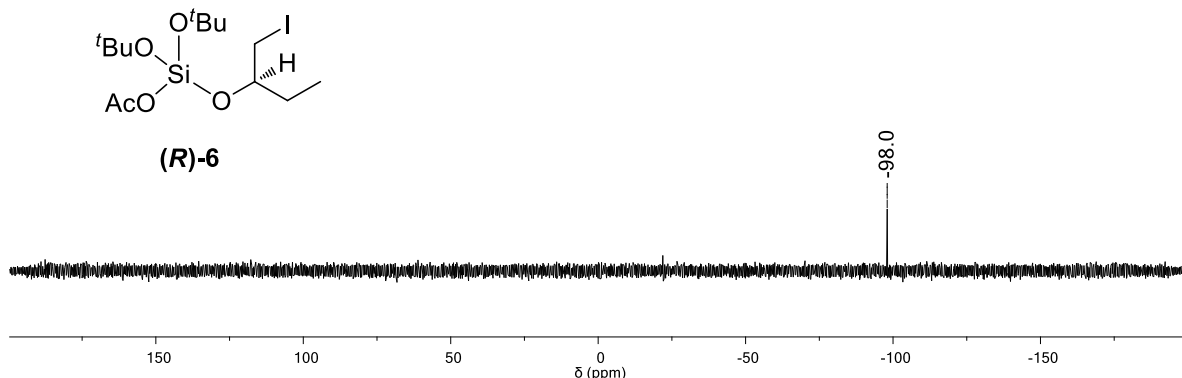


Fig. S18 ^{29}Si NMR spectrum of compound (R) -6.

^1H RMN (300 MHz, CDCl_3)

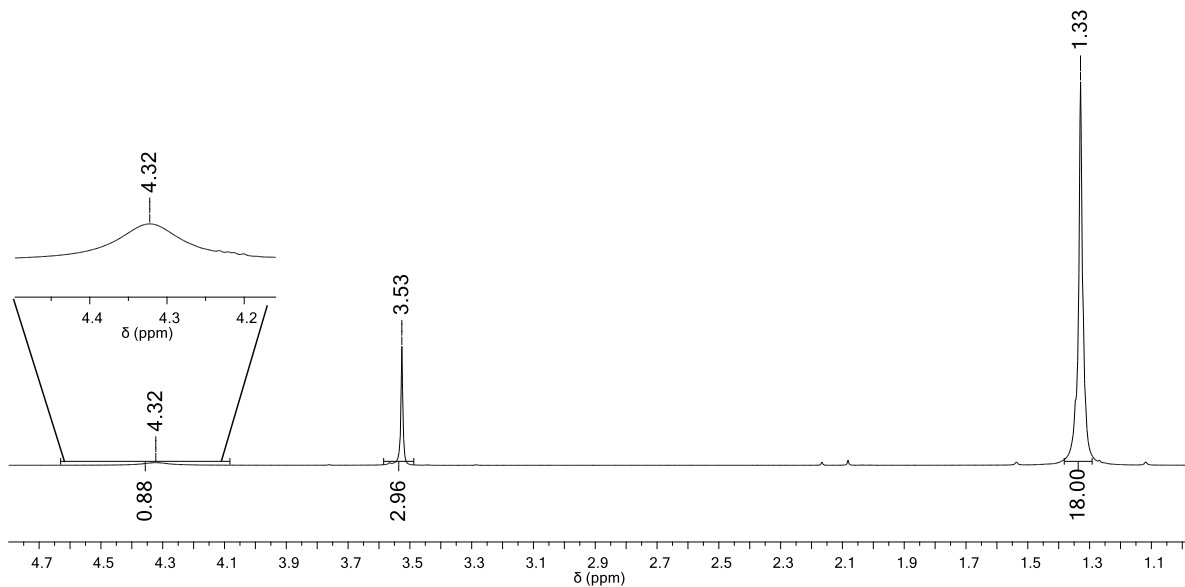
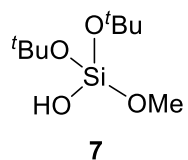


Fig. S19 ^1H NMR spectrum of compound 7.

^{13}C RMN (75 MHz, CDCl_3)

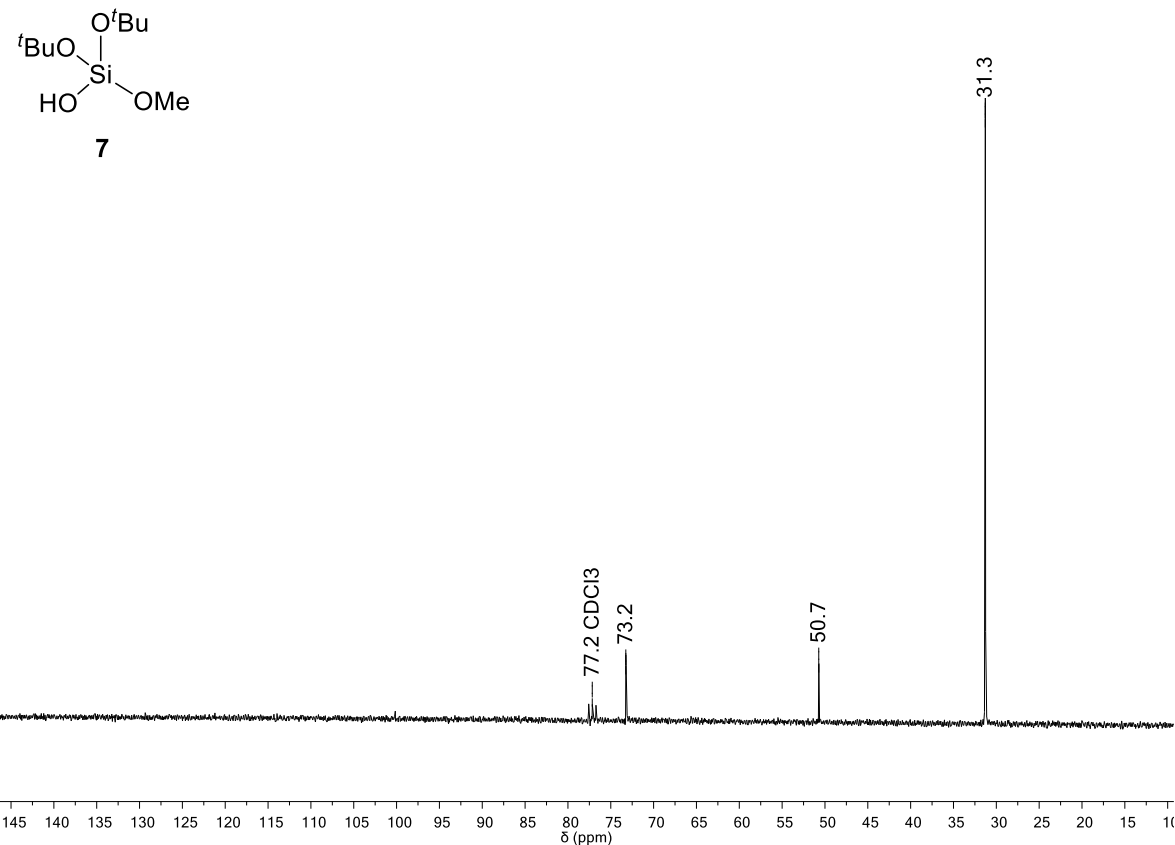


Fig. S20 ^{13}C NMR spectrum of compound 7.

^{29}Si RMN (60 MHz, CDCl_3)

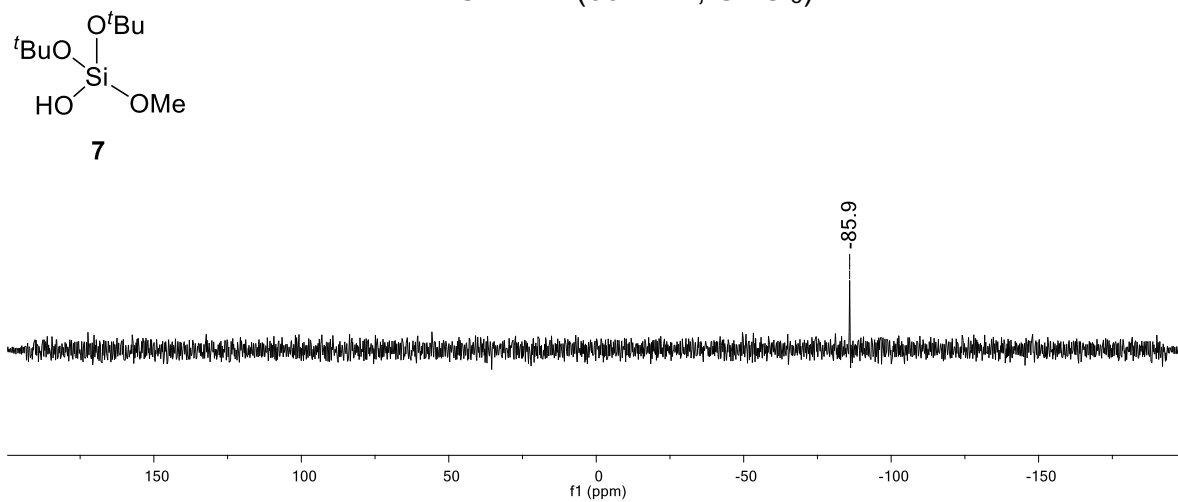


Fig. S21 ^{29}Si NMR spectrum of compound 7.

¹H RMN (300 MHz, CDCl₃)

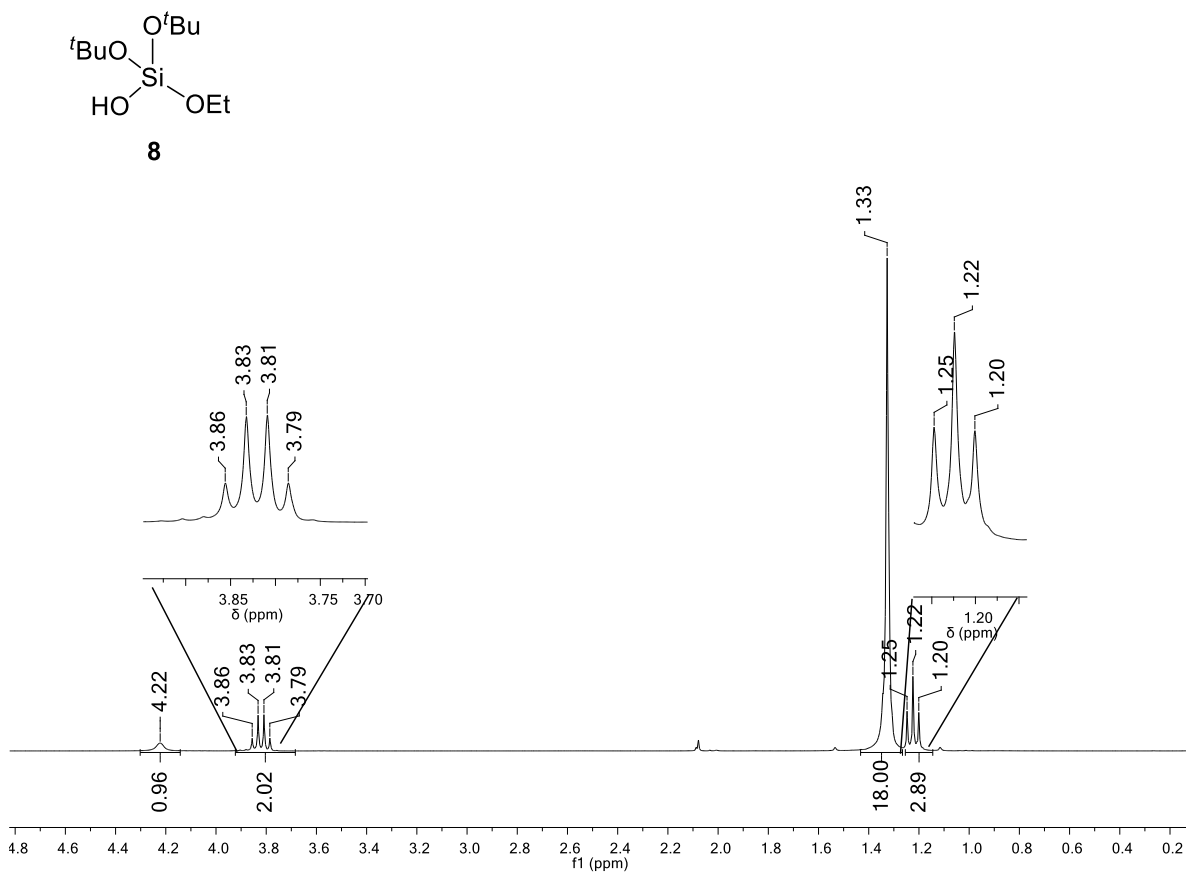


Fig. S22 ¹H NMR spectrum of compound **8**.

^{13}C RMN (75 MHz, CDCl_3)

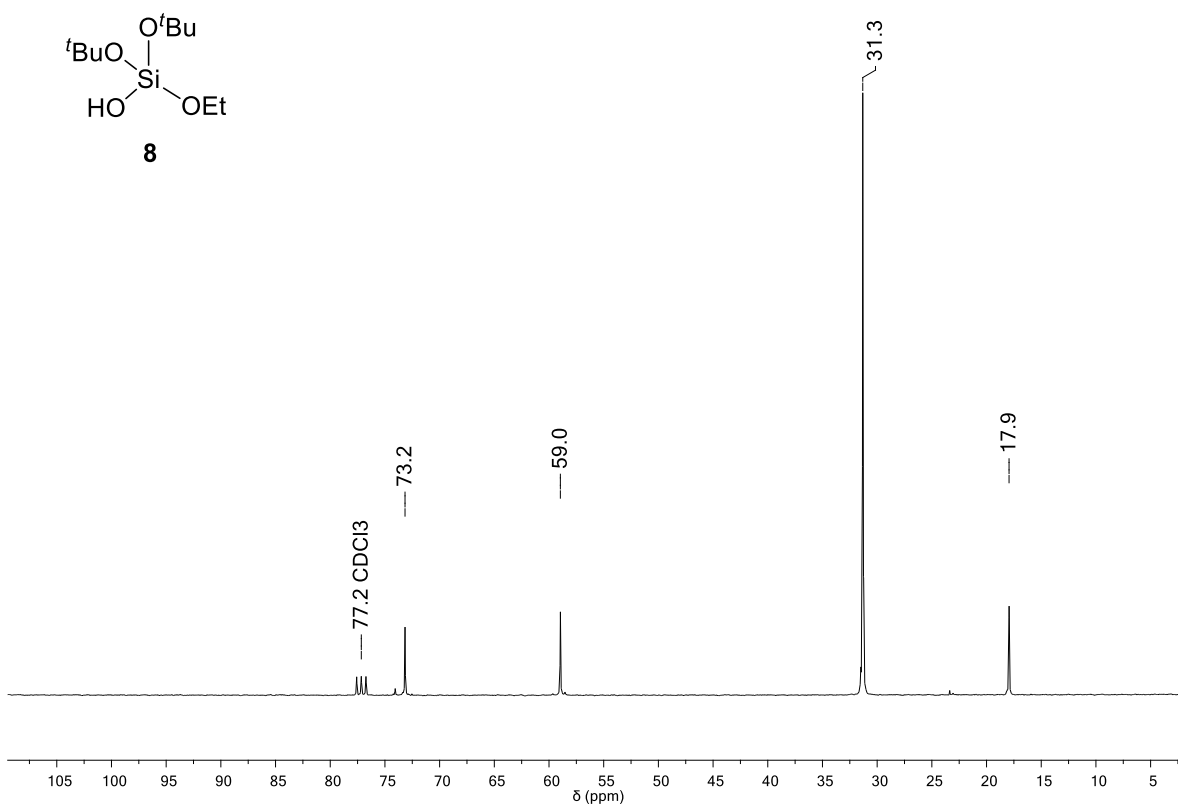


Fig. S23 ^{13}C NMR spectrum of compound 8.

^{29}Si RMN (60 MHz, CDCl_3)

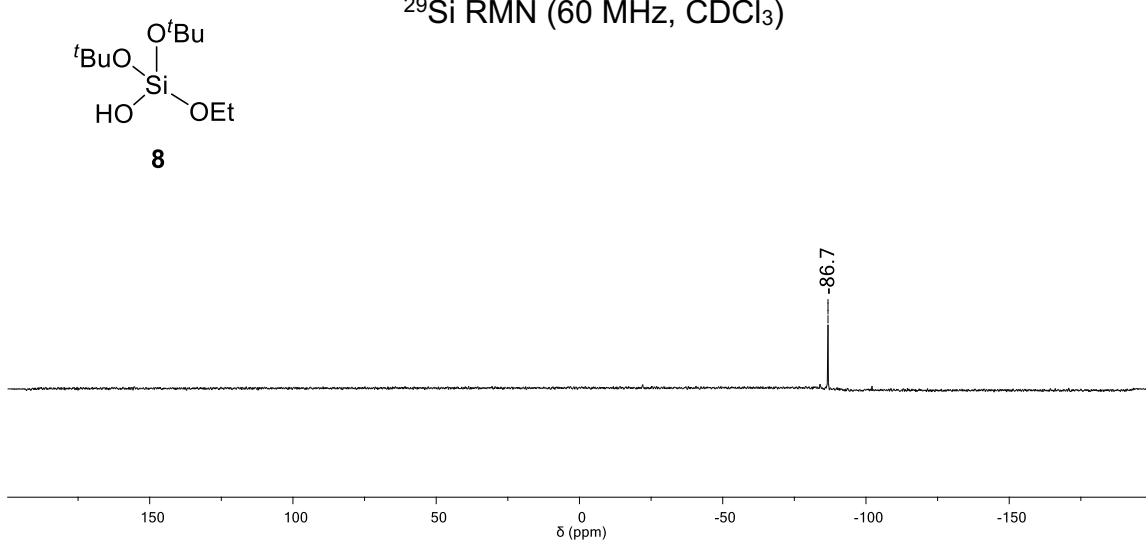


Fig. S24 ^{29}Si NMR spectrum of compound 8.

¹H RMN (300 MHz, CDCl₃)

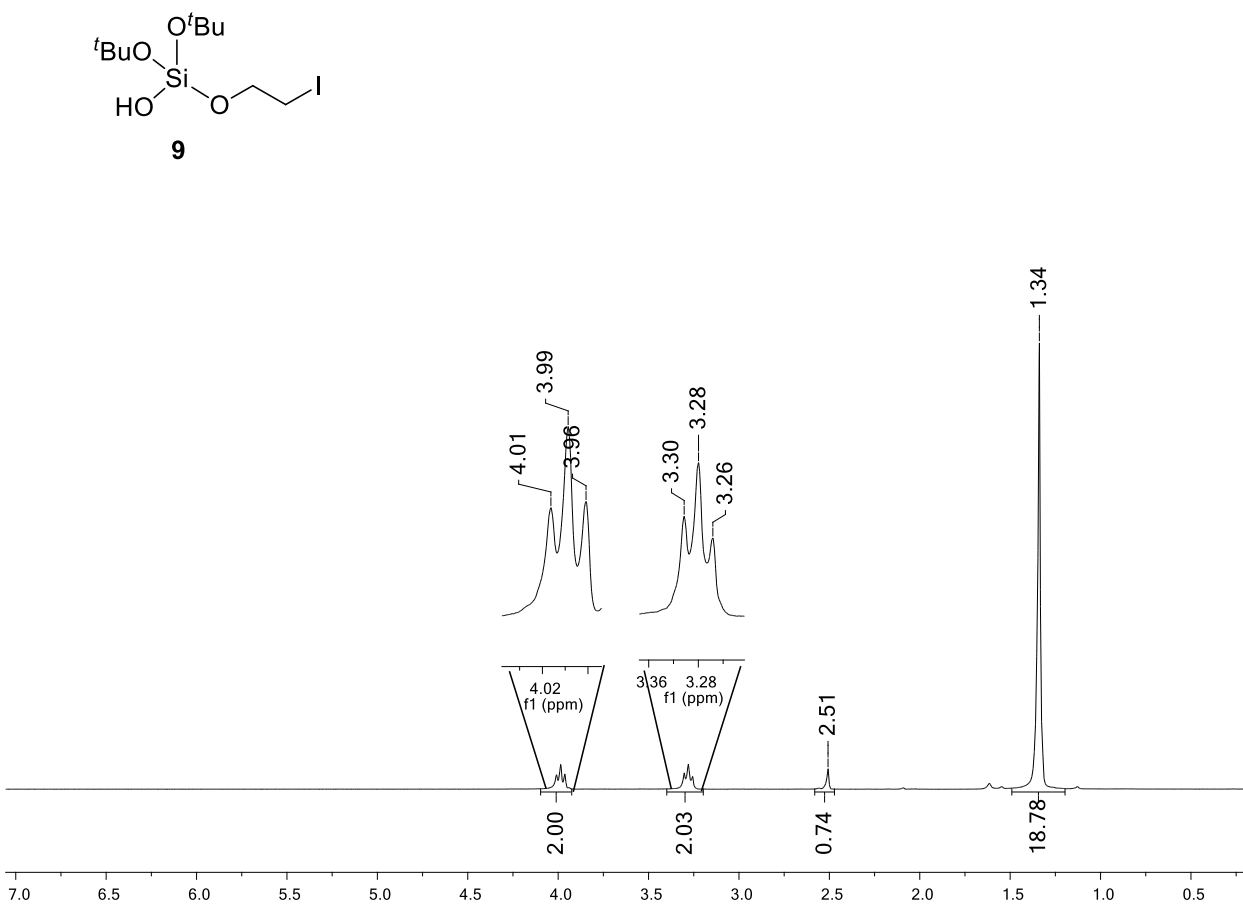


Fig. S25 ¹H NMR spectrum of compound **9**.

^{13}C RMN (75 MHz, CDCl_3)

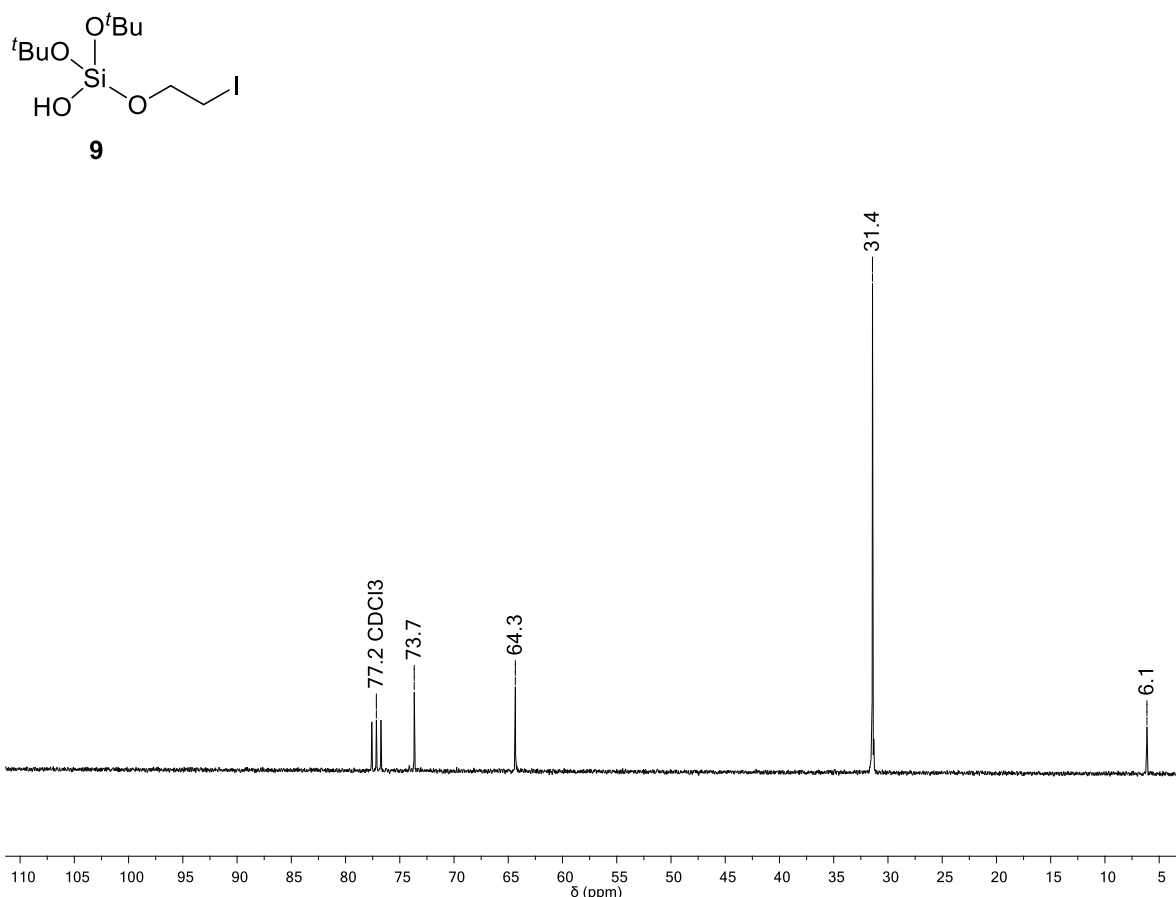


Fig. S26 ^{13}C NMR spectrum of compound **9**.

^{29}Si RMN (60 MHz, CDCl_3)

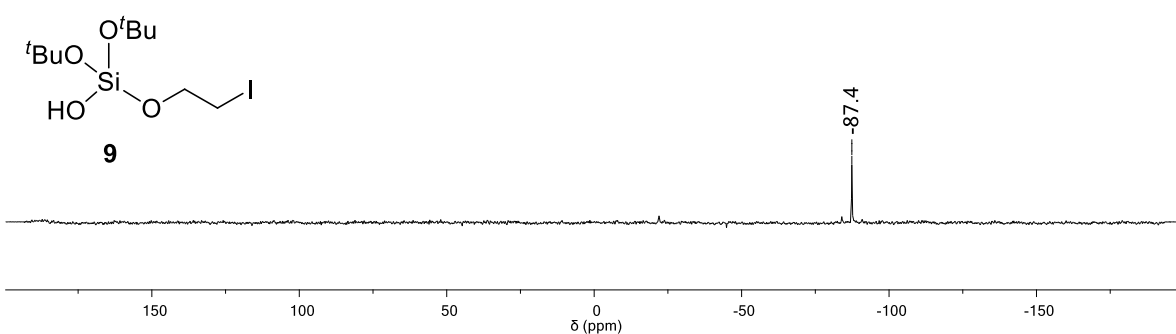


Fig. S27 ^{29}Si NMR spectrum of compound **9**.

^1H RMN (300 MHz, CDCl_3)

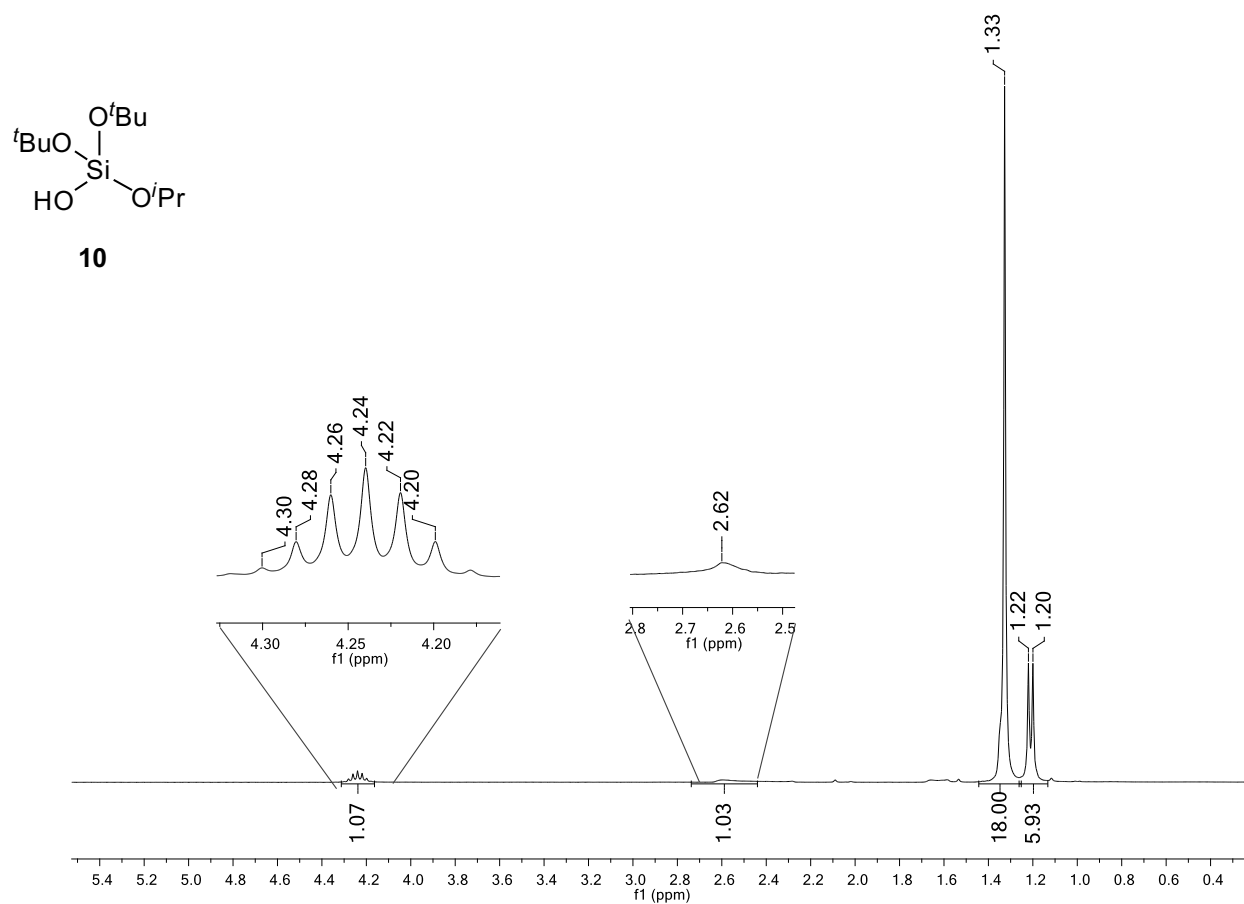


Fig. S28 ^1H NMR spectrum of compound **10**.

^{13}C RMN (75 MHz, CDCl_3)

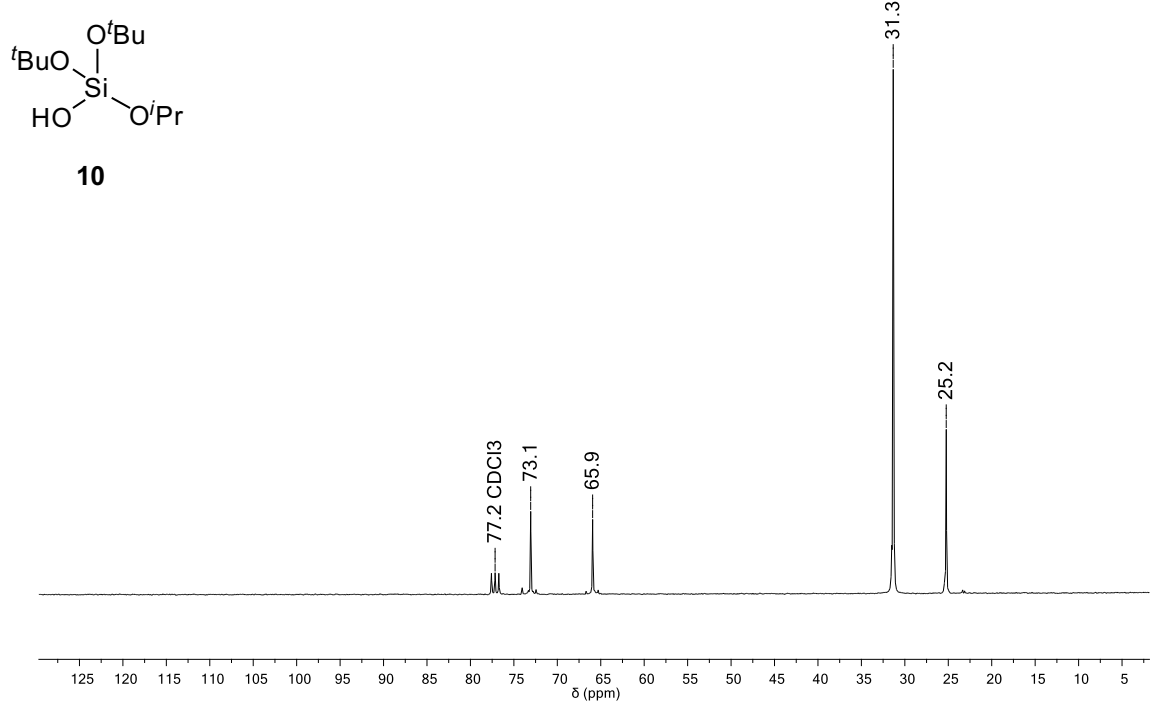


Fig. S29 ^{13}C NMR spectrum of compound **10**.

^{29}Si RMN (60 MHz, CDCl_3)

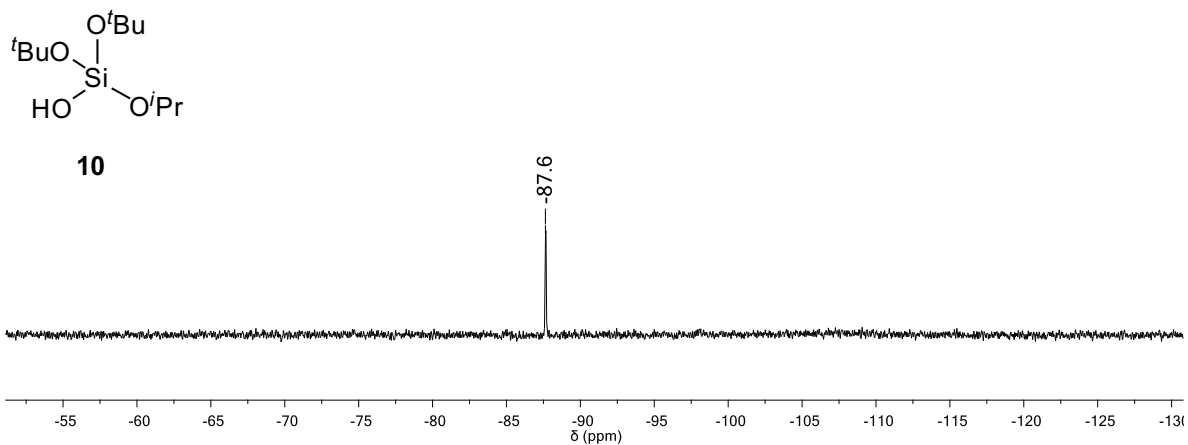


Fig. S30 ^{29}Si NMR spectrum of compound **10**.

¹H RMN (300 MHz, CDCl₃)

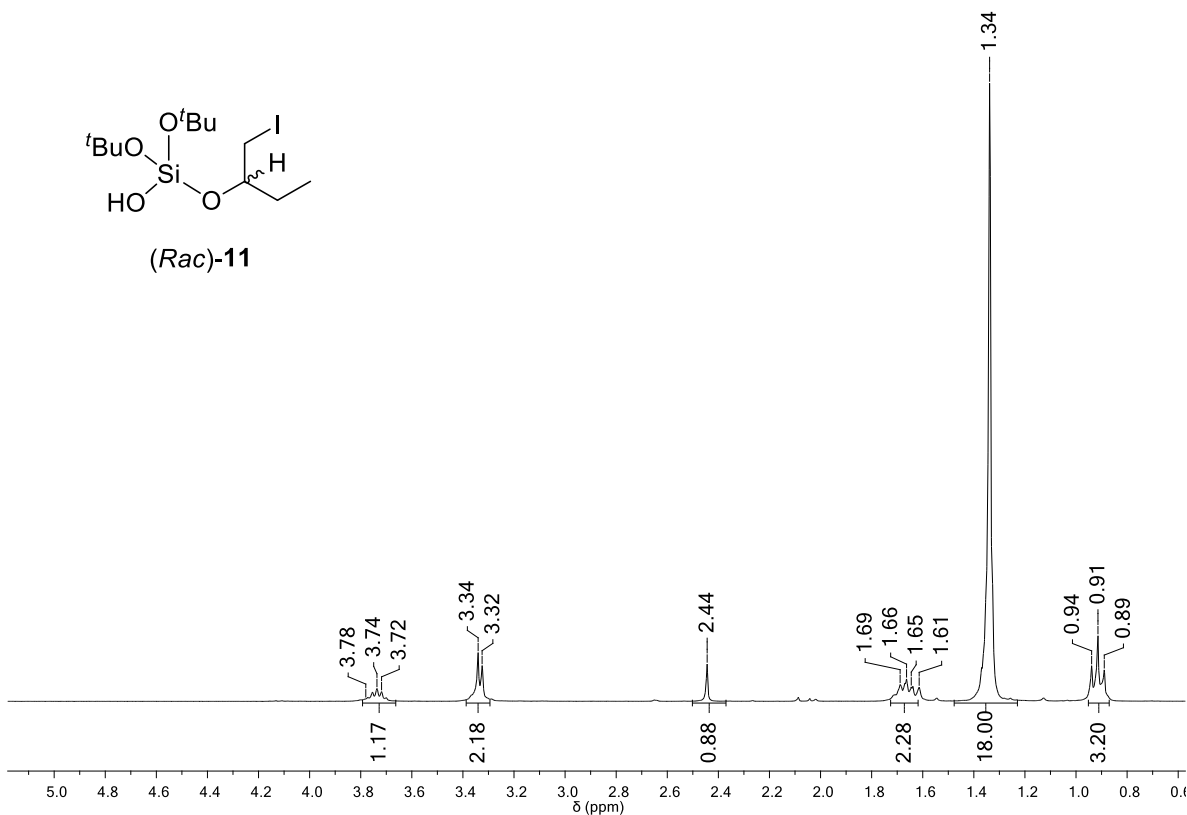


Fig. S31 ¹H NMR spectrum of compound (Rac)-11.

^{13}C RMN (75 MHz, CDCl_3)

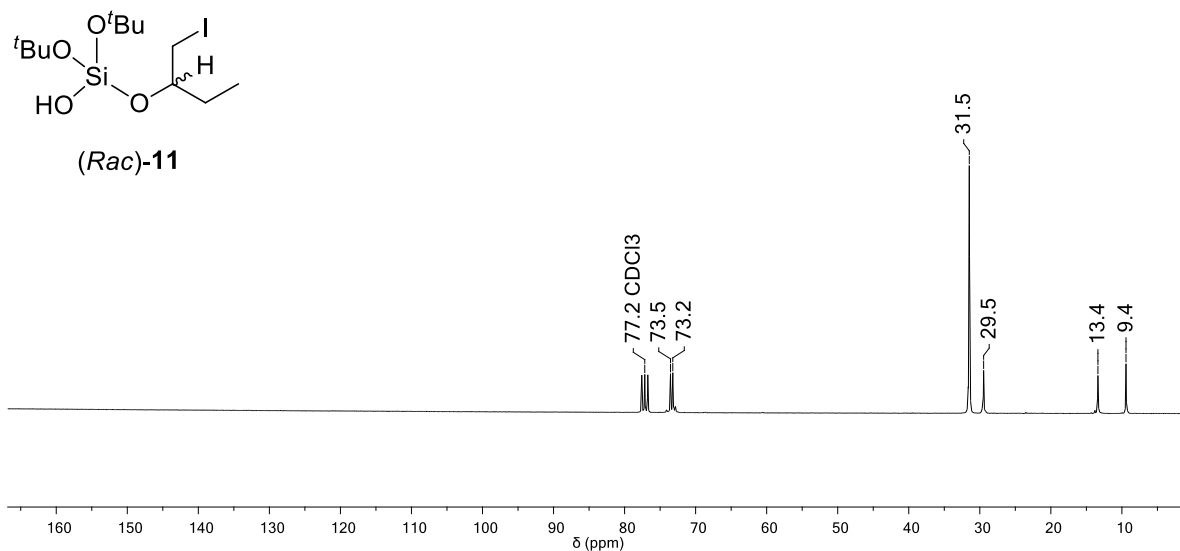


Fig. S32 ^{13}C NMR spectrum of compound (Rac)-11.

^{29}Si RMN (60 MHz, CDCl_3)

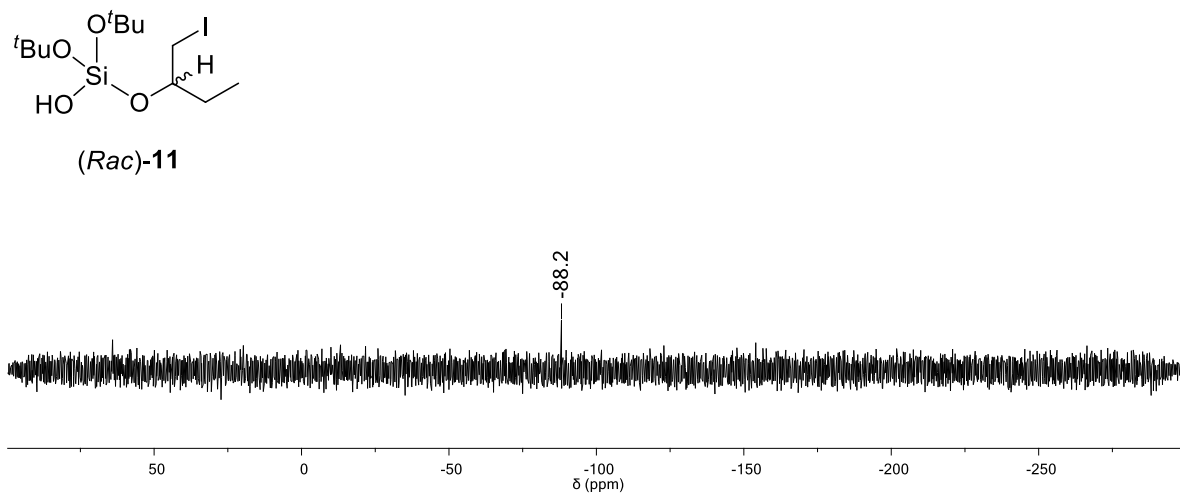


Fig. S33 ^{29}Si NMR spectrum of compound (Rac)-11.

^1H RMN (300 MHz, CDCl_3)

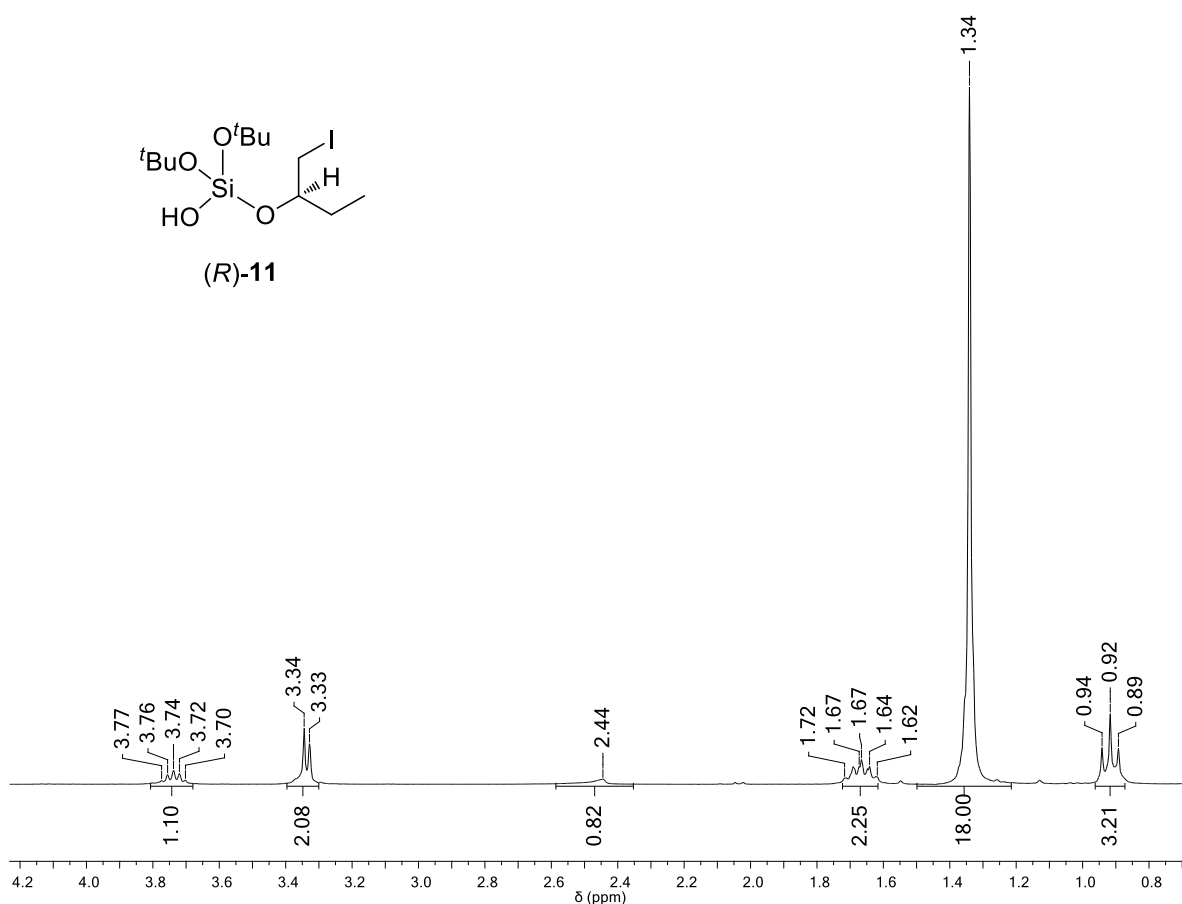


Fig. S34 ^1H NMR spectrum of compound (R) -11.

^{13}C RMN (75 MHz, CDCl_3)

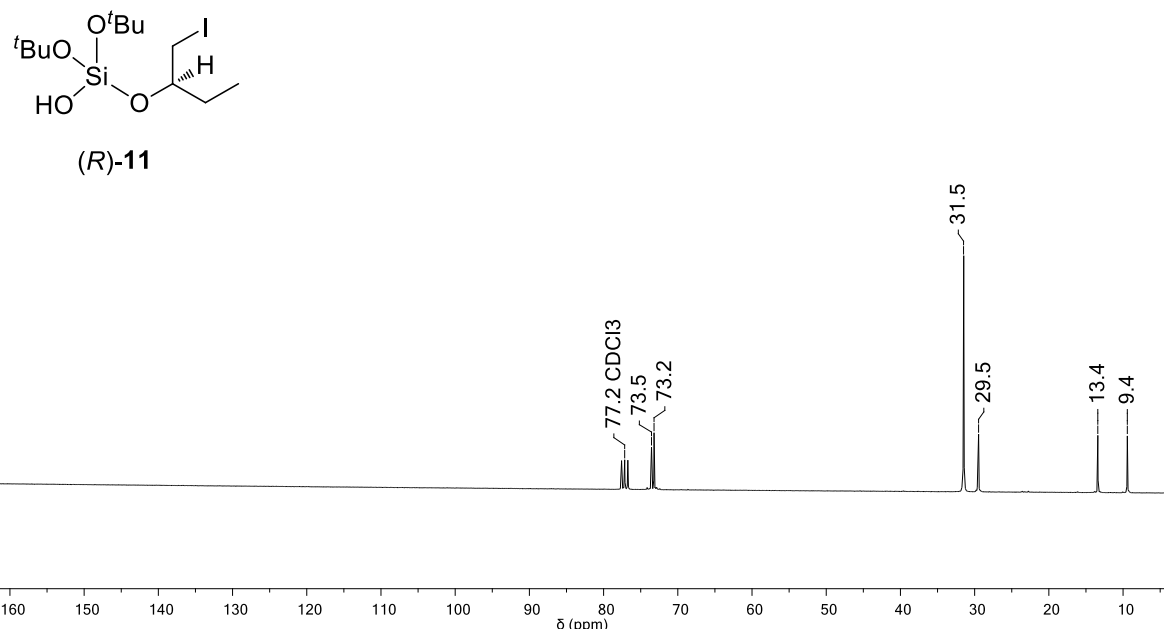


Fig. S35 ^{13}C NMR spectrum of compound (R) -11.

^{29}Si RMN (60 MHz, CDCl_3)

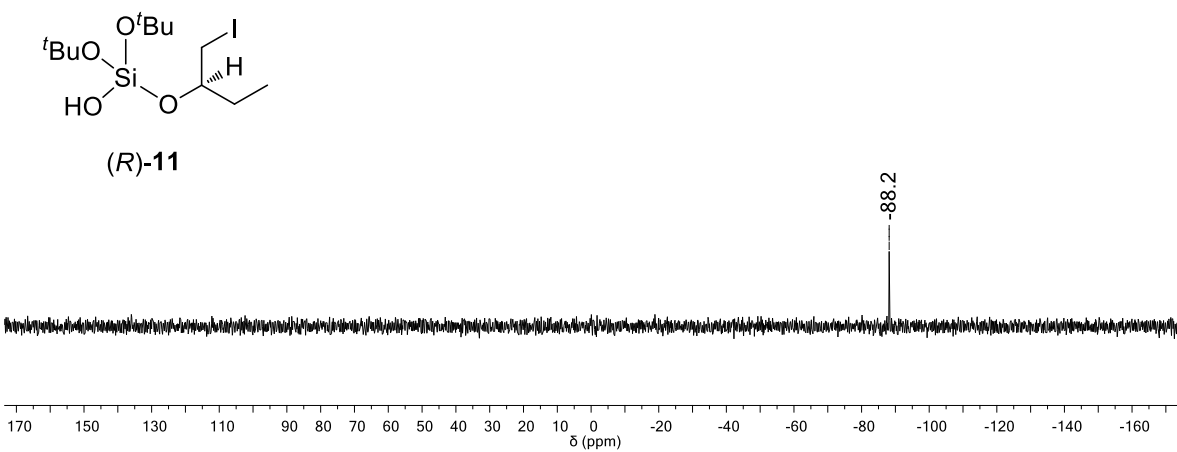


Fig. S36 ^{29}Si NMR spectrum of compound (R) -11.

^1H RMN (300 MHz, CDCl_3)

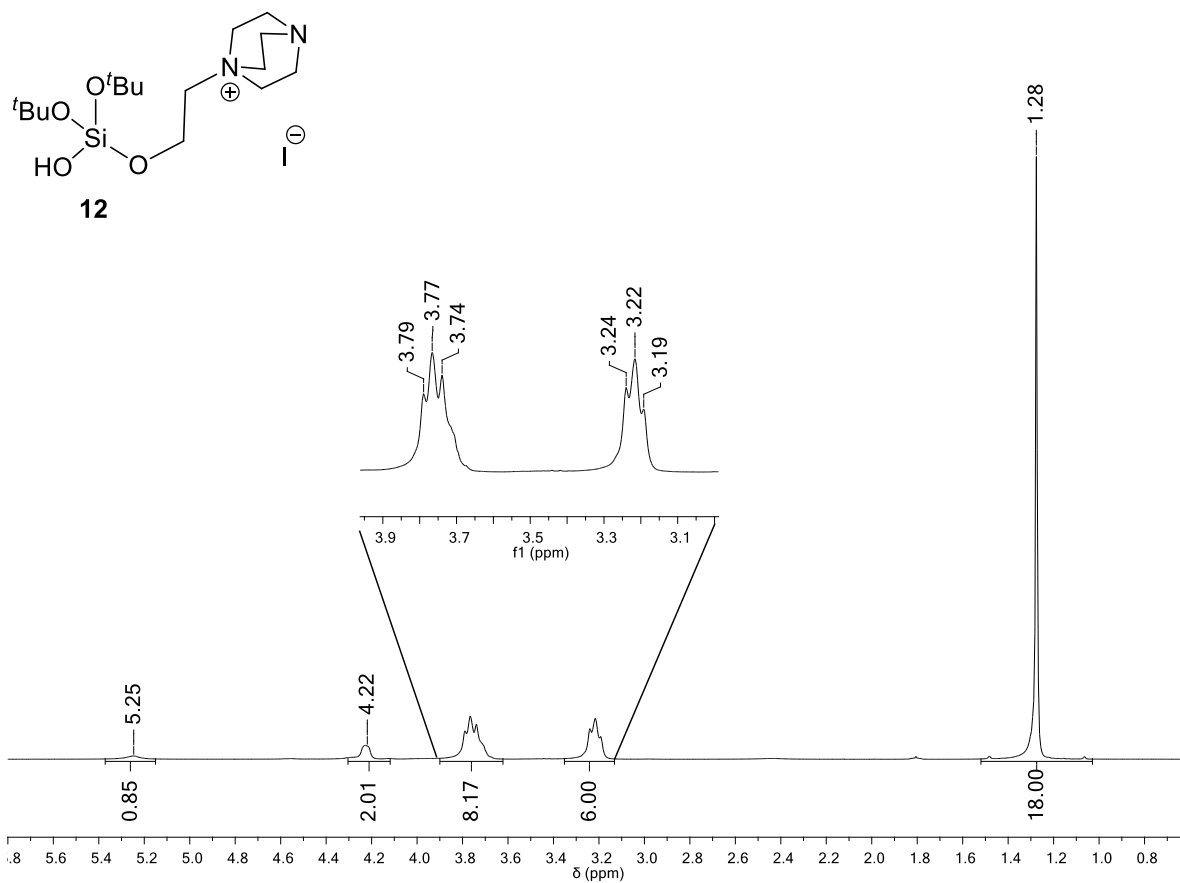


Fig. S37 ^1H NMR spectrum of compound **12**.

^{13}C RMN (75 MHz, CDCl_3)

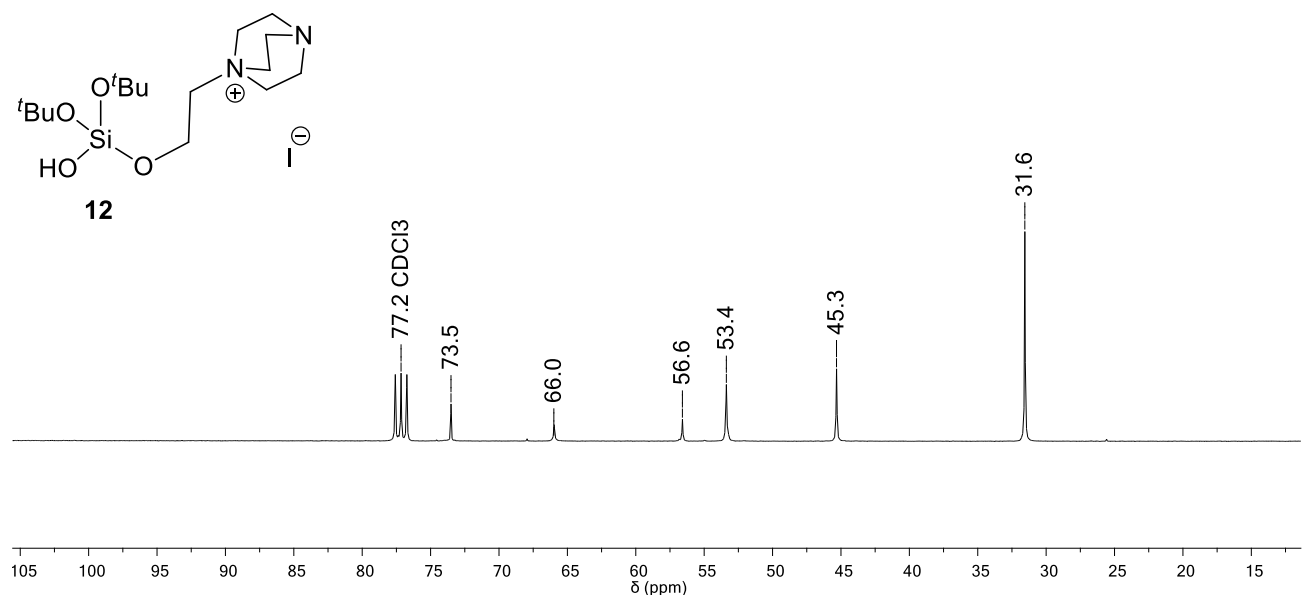


Fig. S38 ^{13}C NMR spectrum of compound **12**.

^{29}Si RMN (60 MHz, CDCl_3)

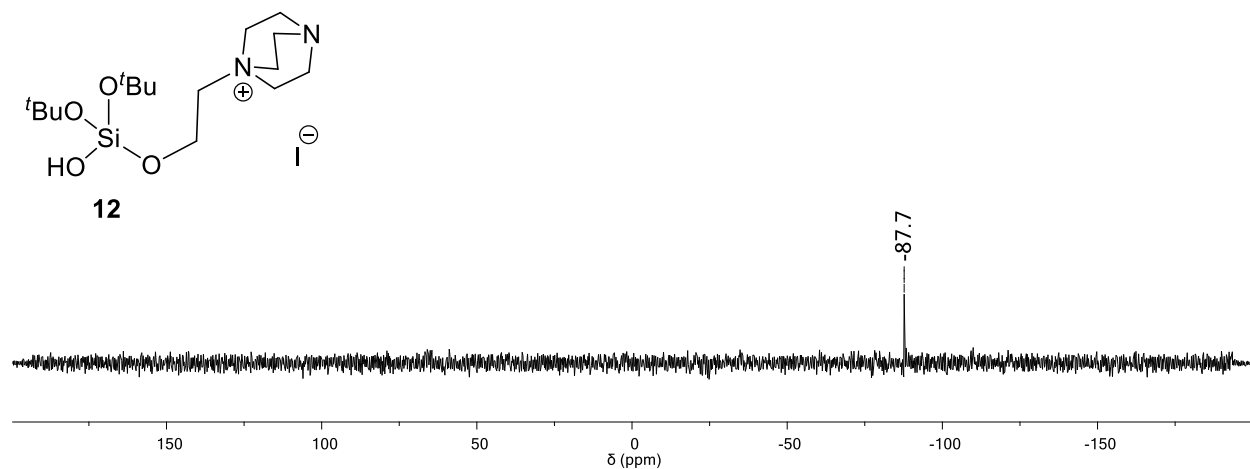


Fig. S39 ^{29}Si NMR spectrum of compound **12**.

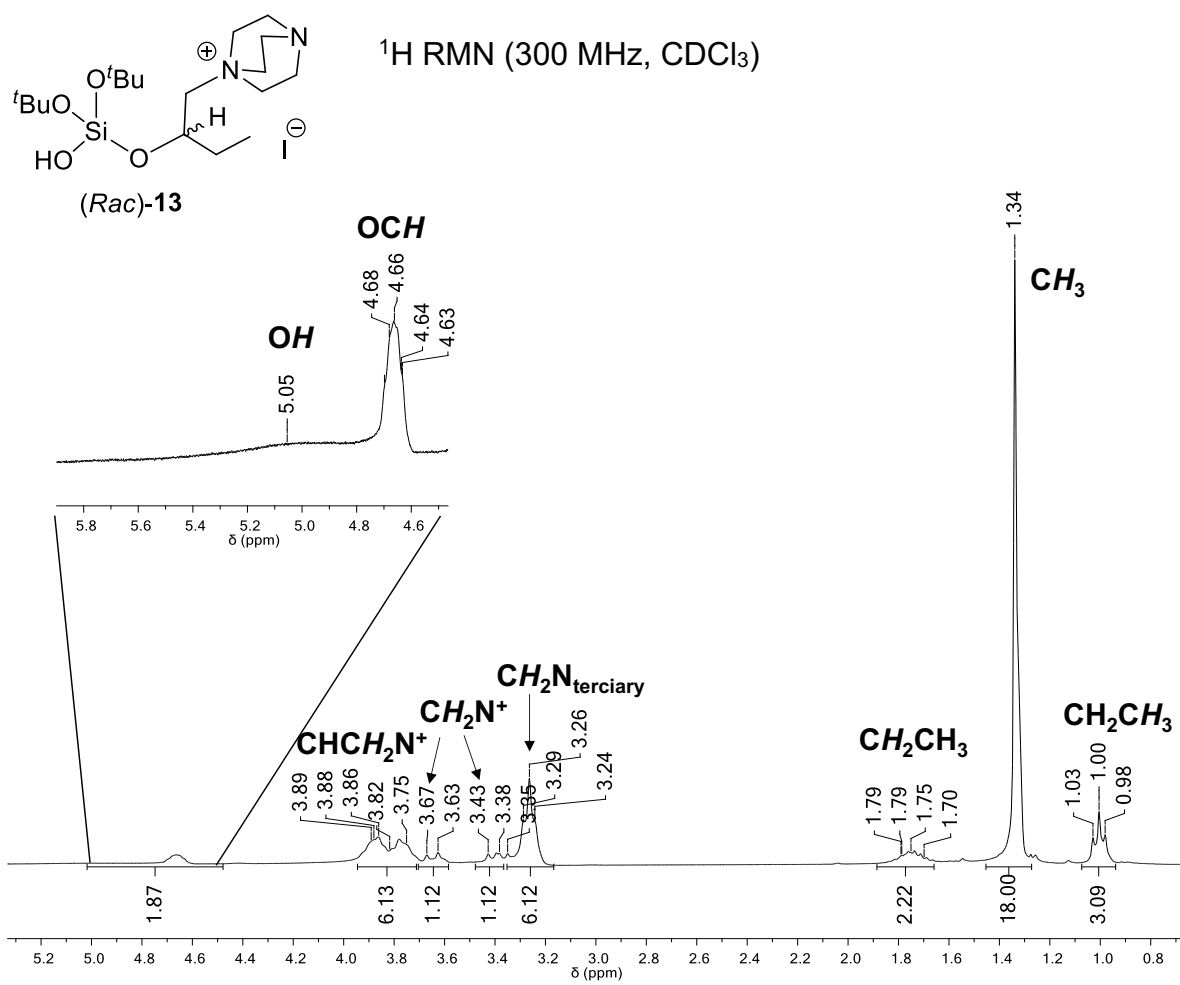
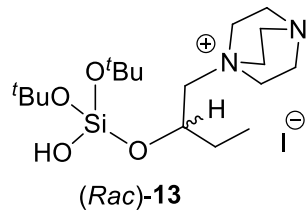


Fig. S40 ¹H NMR spectrum of compound *(Rac)-13*.

^{13}C RMN (75 MHz, CDCl_3)



(Rac)-13

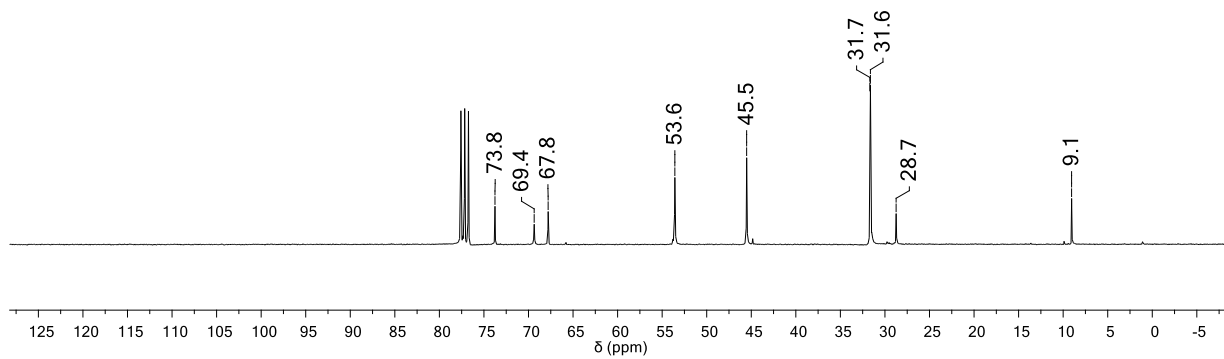
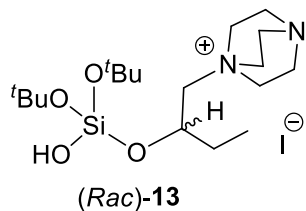


Fig. S41 ^{13}C NMR spectrum of compound (Rac)-13.

^{29}Si RMN (60 MHz, CDCl_3)



(Rac)-13

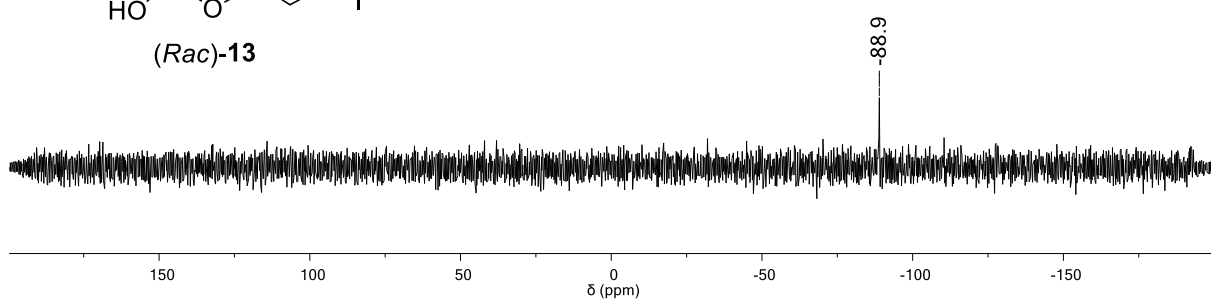


Fig. S42 ^{29}Si NMR spectrum of compound (Rac)-13.

^1H RMN (300 MHz, CDCl_3)

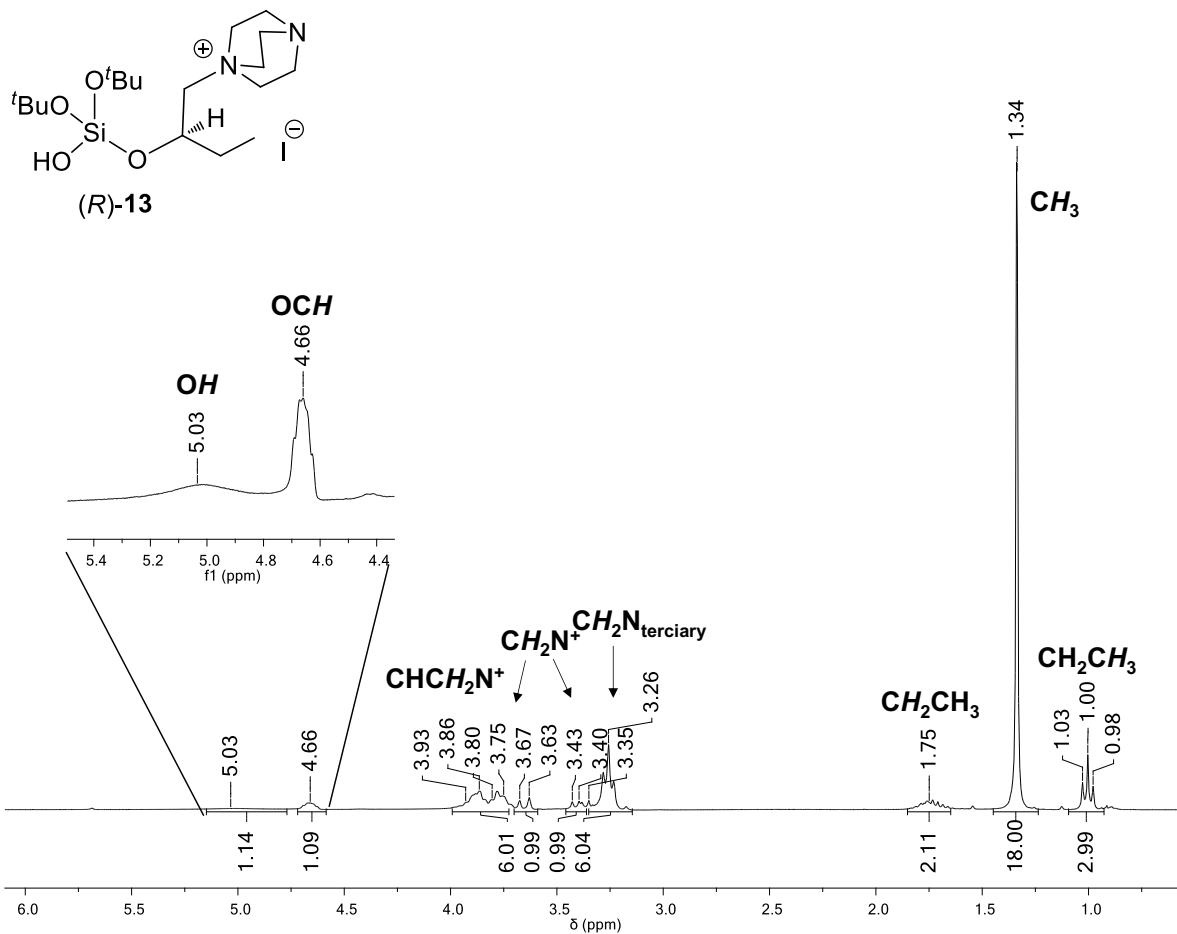


Fig. S43 ^1H NMR spectrum of compound (*R*)-13.

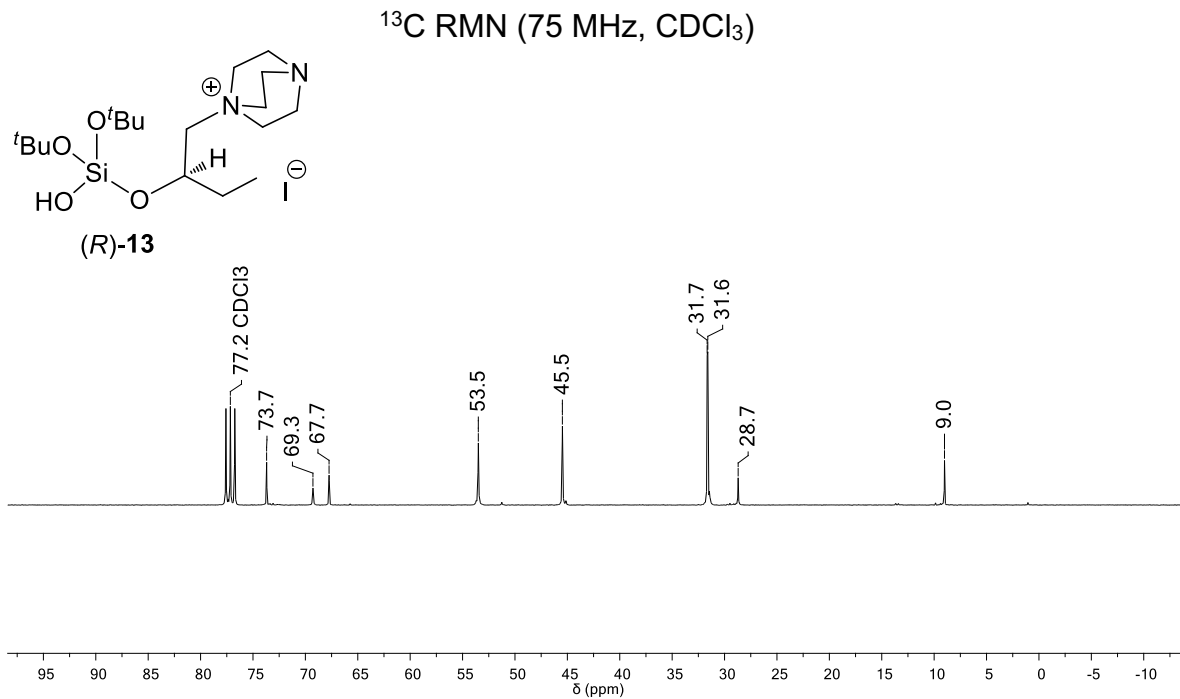


Fig. S44 ¹³C NMR spectrum of compound (R)-13.

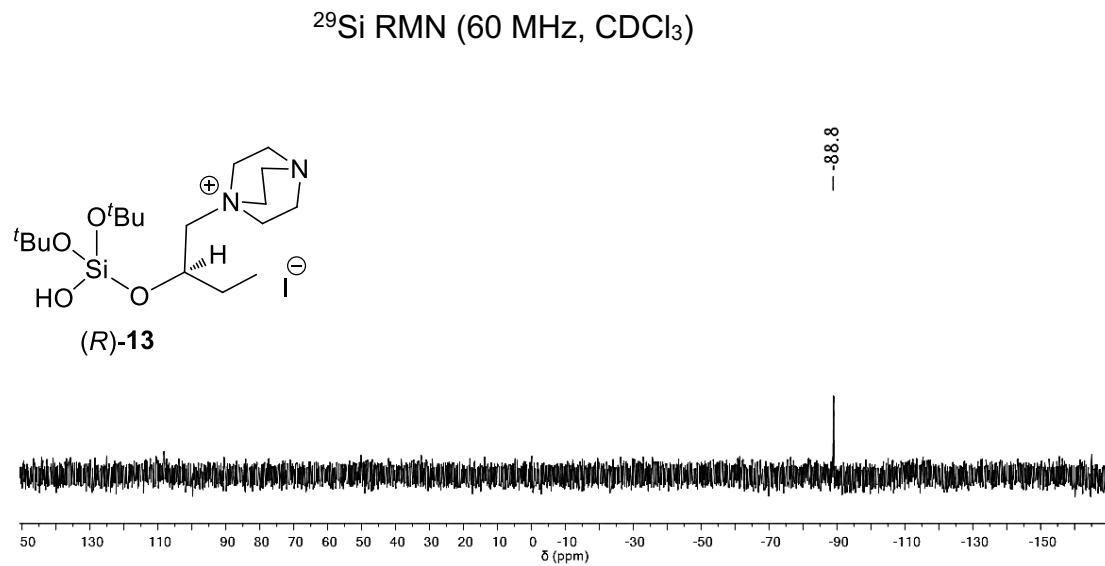
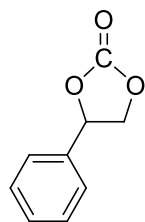


Fig. S45 ²⁹Si NMR spectrum of compound (R)-13.

^1H RMN (500 MHz, CDCl_3)



15a

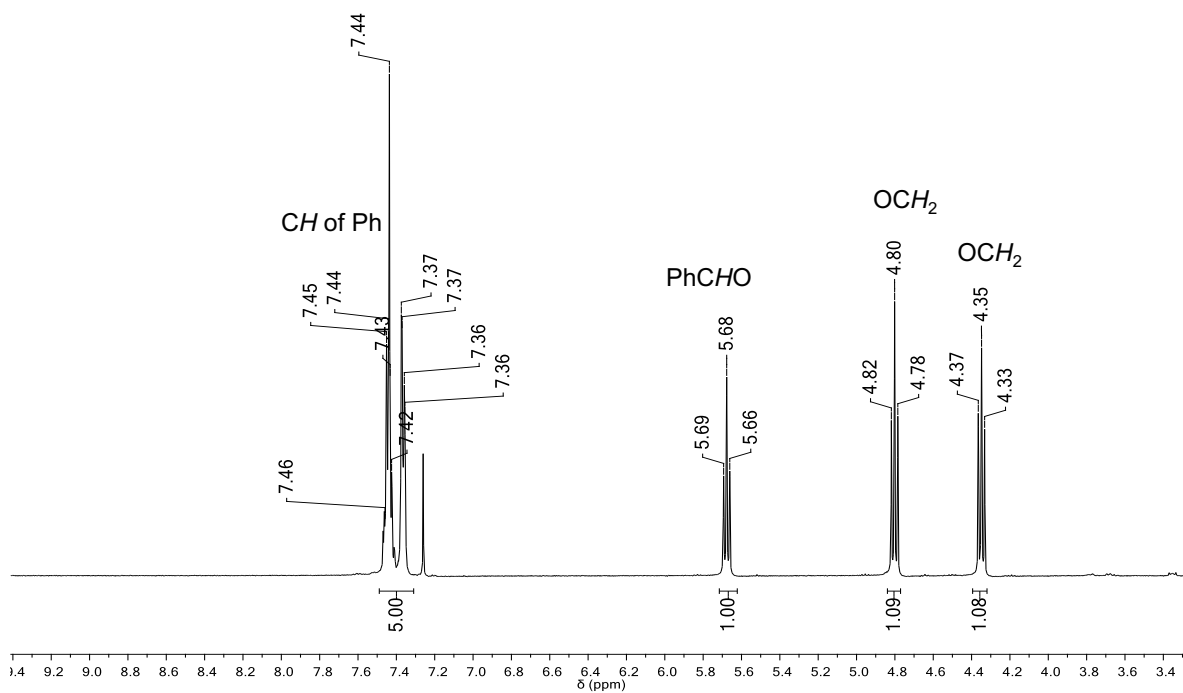


Fig. S46 ^1H NMR spectrum of styrene carbonate **15a**.

^1H RMN (300 MHz, CDCl_3)

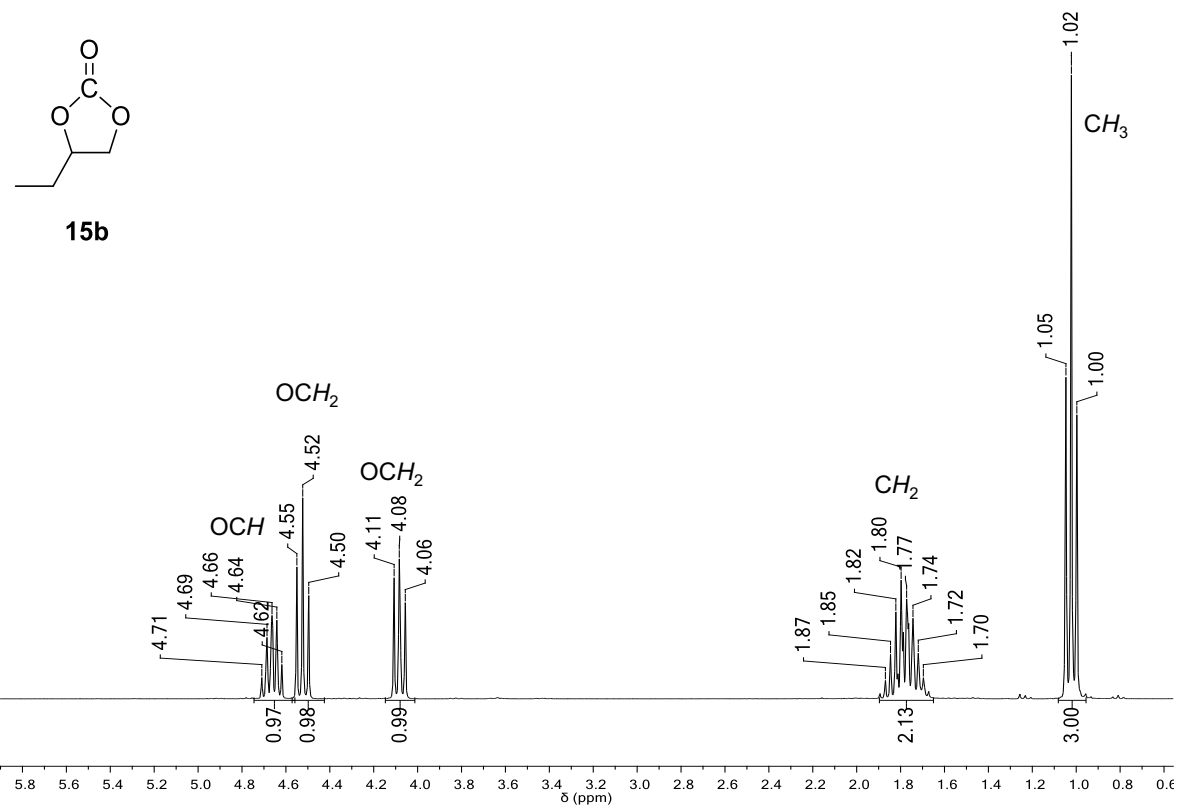


Fig. S47 ^1H NMR spectrum of (*Rac*)-1,2-butylene carbonate **15b**.

¹H RMN (500 MHz, CDCl₃)

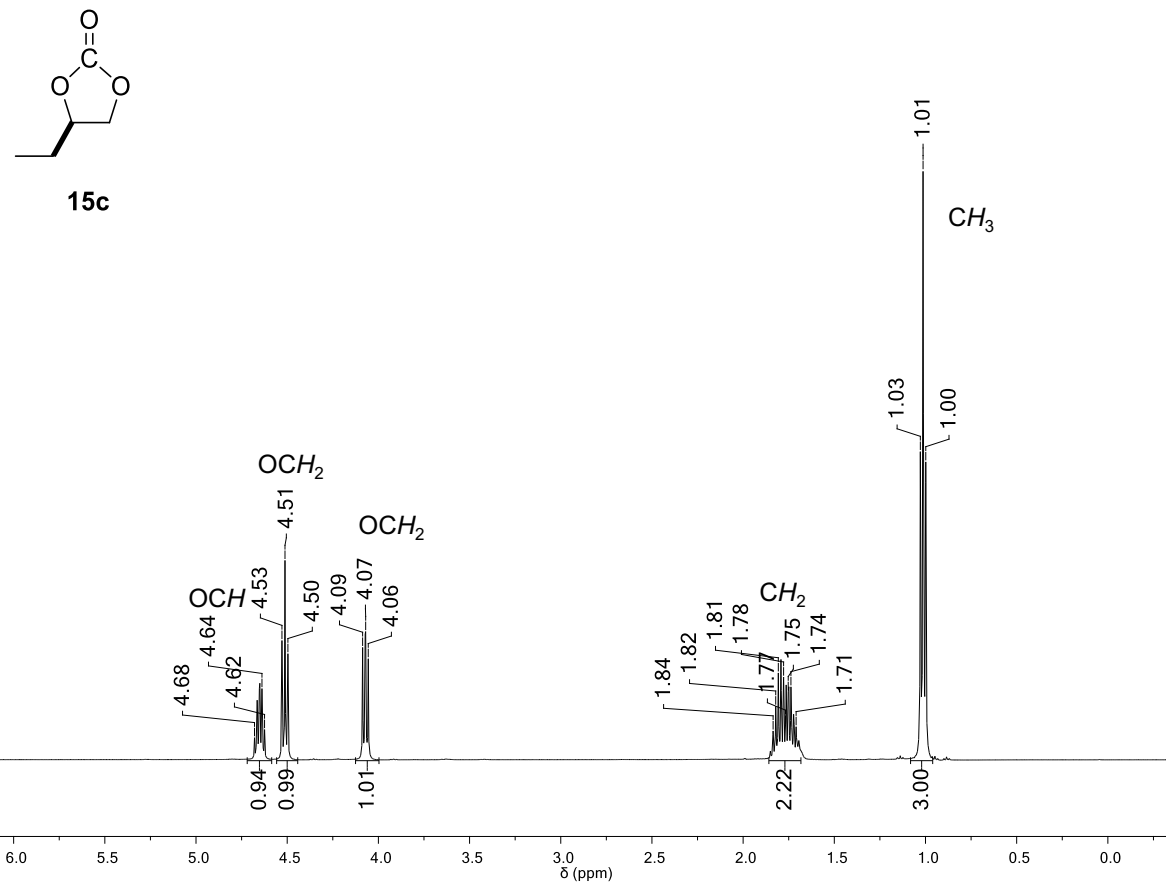


Fig. S48 ¹H NMR spectrum of (*R*)-1,2-butylene carbonate **15c**.

^1H RMN (300 MHz, CDCl_3)

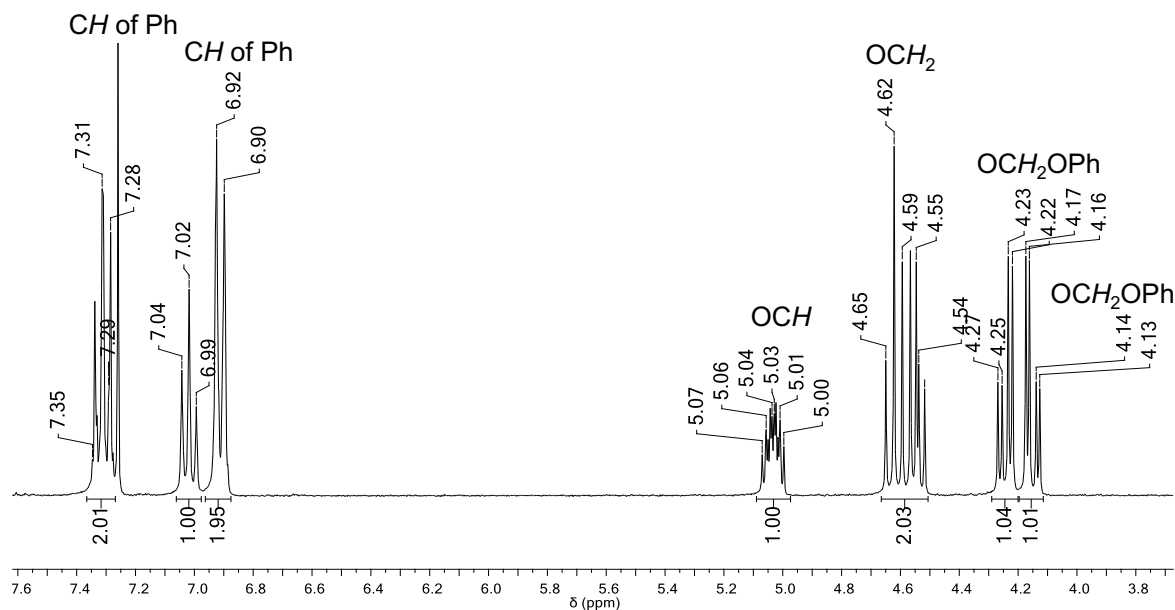
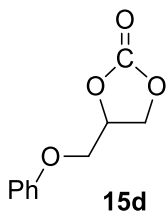


Fig. S49 ^1H NMR spectrum of 3-phenoxypropylene carbonate **15d**.

^1H RMN (300 MHz, CDCl_3)

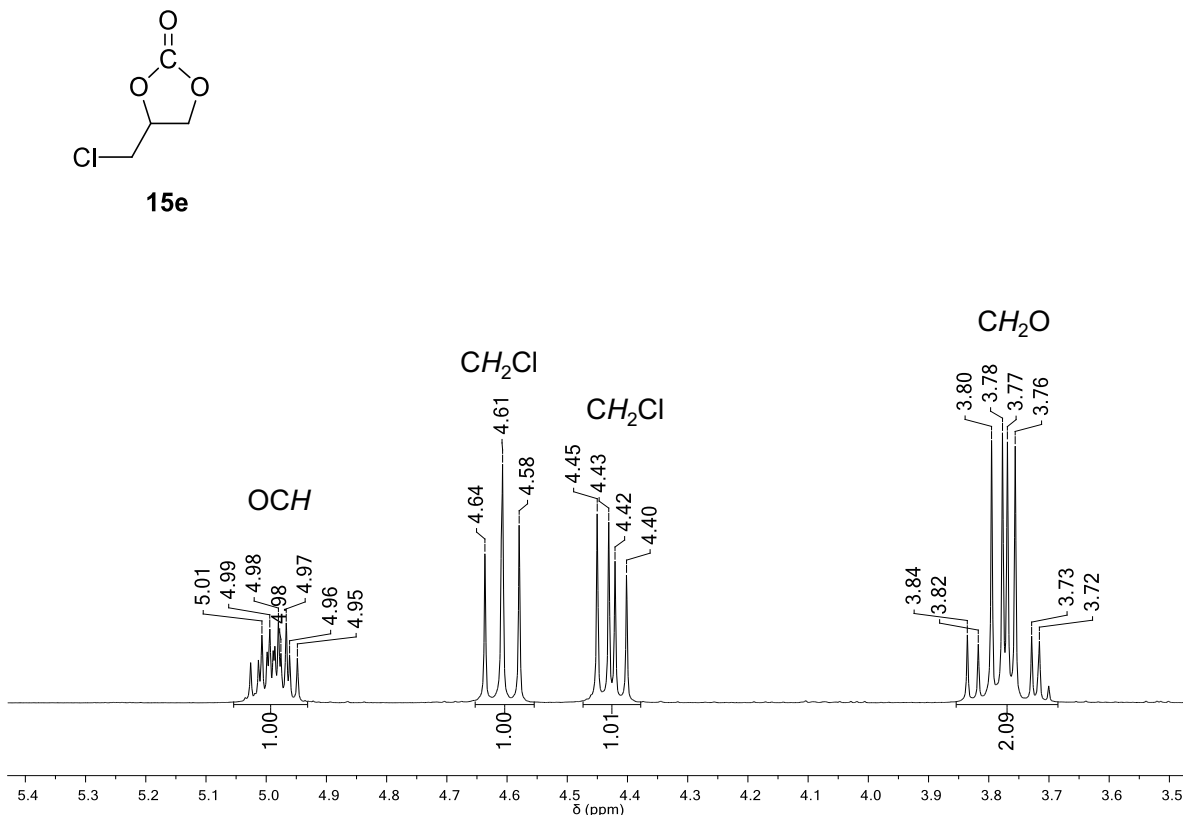


Fig. S50 ^1H NMR spectrum of 3-chloropropylene carbonate **15e**.

^1H RMN (300 MHz, CDCl_3)

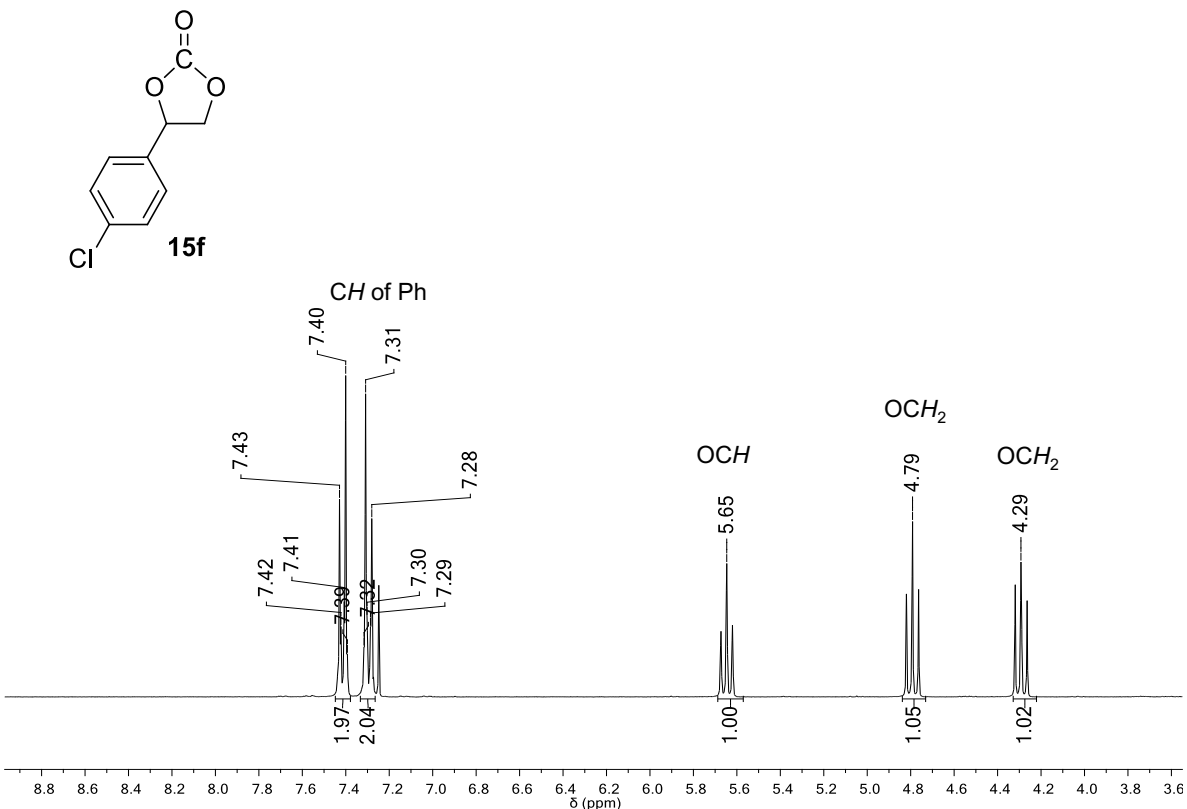


Fig. S51 ^1H NMR spectrum of 4-chlorostyrene carbonate **15f**.

^1H RMN (500 MHz, CDCl_3)

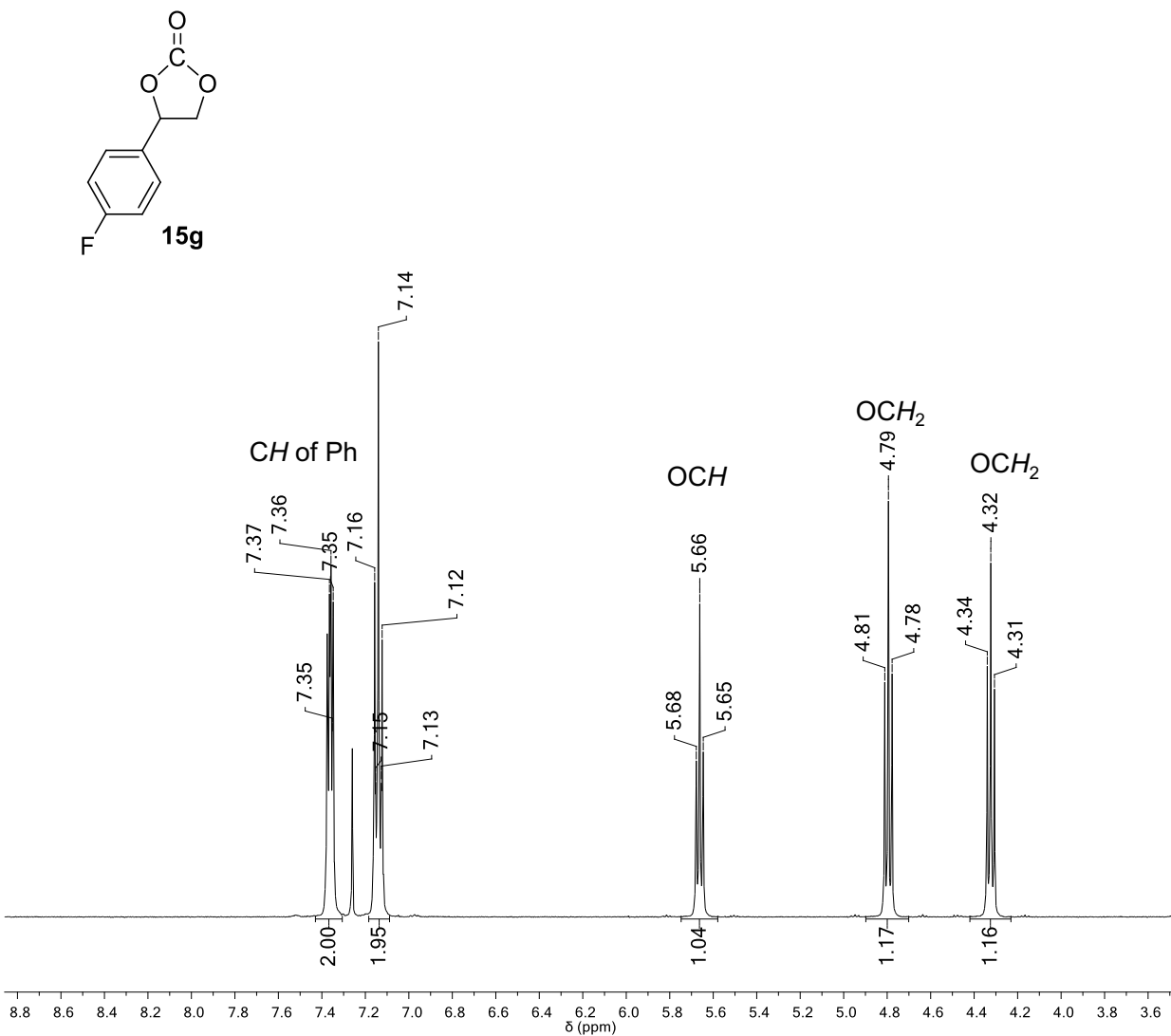


Fig. S52 ^1H NMR spectrum of 4-fluorostyrene carbonate **15g**.

^1H RMN (500 MHz, CDCl_3)

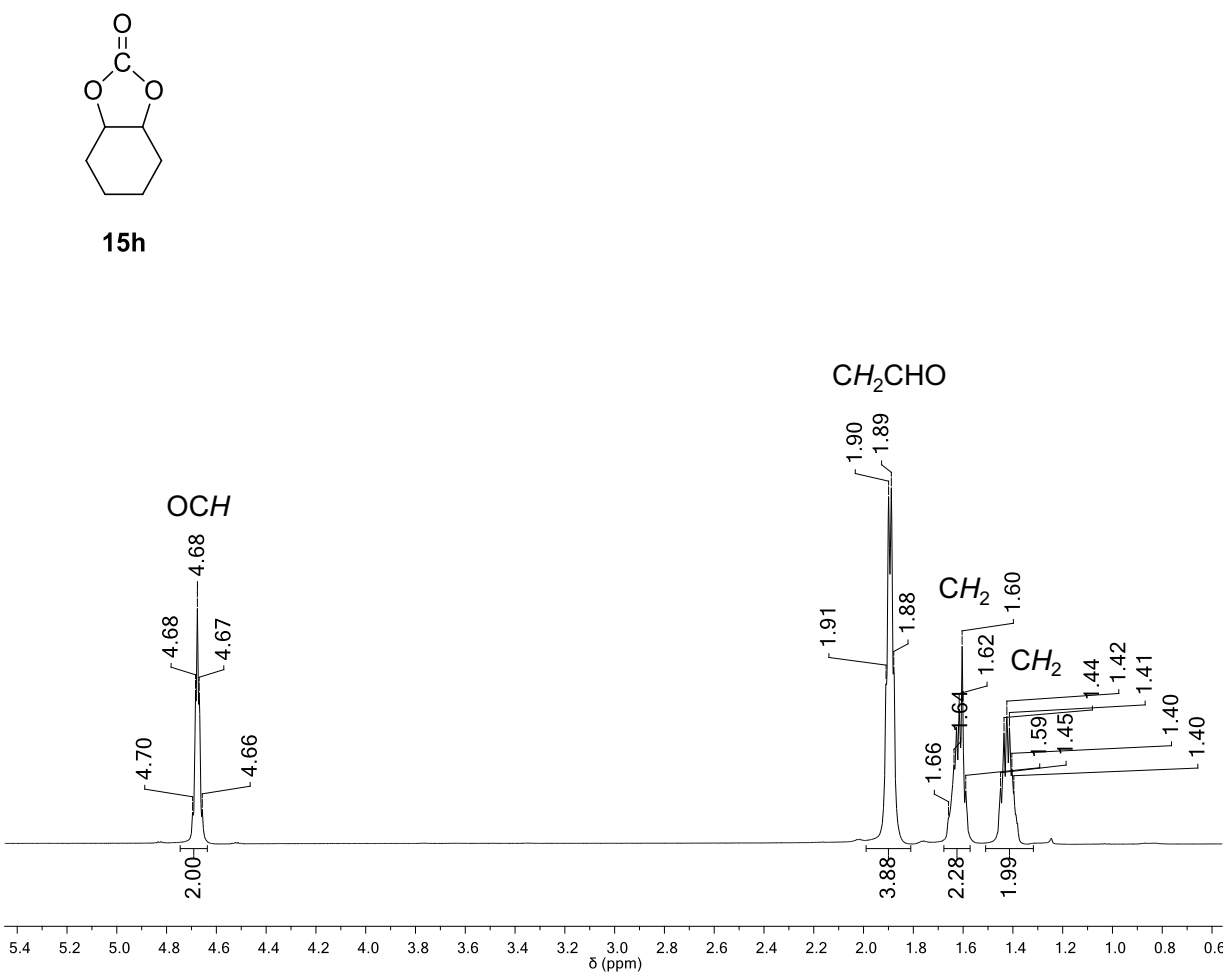


Fig. S53 ^1H NMR spectrum of cyclohexene carbonate **15h**.

Metal-free catalysts in the synthesis of cyclic carbonates

Large number of metal-free catalysts active in the CO₂ activation reactions has been described, but there are no unified reaction conditions and making a direct comparison of **12** and **13** with literature is difficult. Therefore, Table S1 contains some examples of bifunctional catalysts that show good catalytic activity in CO₂ activation and are based on quaternary phosphonium salts,^{1,2} carboxylic acids,³ and ionic liquids.^{4,5} However, in most cases, high pressures and/or temperatures^{3,4} or high catalyst loads (10-15% mol)² are required. In our case, the bifunctional silanol-based catalysts have a good catalytic activity using low pressures and temperatures below 100 ° C.

Furthermore, compared to previously described silanol-based catalysts,^{6,7} compounds **12** and **13** are air- and moisture-stable facilitating their handling and storage. Also, bifunctional silanols **12** and **13** show good to a very good conversion of epoxides to the corresponding cyclic carbonates, with low catalyst loads (4 % mol) and in the absence of an external nucleophile source.

Table S1 Selected highly active catalysts for the cycloaddition of epoxides and CO₂.

Ref.	Compound	Reaction conditions
1		<ul style="list-style-type: none"> • 1 atm CO₂ in chlorobenzene at 120 °C for 12 h. • Catalyst loading 15 mol%
2		<ul style="list-style-type: none"> • 1 atm CO₂ (solvent free) at 60°C for 24 h. • Catalyst loading (1 mol%).
3		<ul style="list-style-type: none"> • 290 psi CO₂ (solvent free) at 130 °C for 1h. • Catalyst loading (1 mol%).
4		<ul style="list-style-type: none"> • 145 psi CO₂ (solvent free) at 80 °C for 1h. • Catalyst loading (1 mol%).
5		<ul style="list-style-type: none"> • 60 psi CO₂ at 70 °C for 16h. • Catalyst loading (5 mol%).
6		<ul style="list-style-type: none"> • 1 atm CO₂ (solvent free) at 25 °C for 18 h. • Catalyst loading (10 mol%) and cocatalyst loading TBAI (10 % mol).
7		<ul style="list-style-type: none"> • 1 atm CO₂ (solvent free) at 60°C for 15 h. • Catalyst loading (10 mol%) and cocatalyst loading TBAI (10 % mol)
This work		<ul style="list-style-type: none"> • 75 psi CO₂ (solvent free) at 60°C for 10 h. • Catalyst loading (4 mol%)

Table S2 Selected crystallographic data for compounds **12**, (*Rac*)-**13** and (*R*)-**13**.

	12	(<i>Rac</i>)- 13	(<i>R</i>)- 13
Empirical formula	C ₁₆ H ₃₅ IN ₂ O ₄ Si	C ₁₈ H ₃₉ IN ₂ O ₄ Si	C ₁₈ H ₃₉ IN ₂ O ₄ Si
Formula mass (g/mol)	474.45	502.50	502.50
T (K)	100(2)	100(2)	100(2)
Crystal size (mm ³)	0.319 x 0.214 x 0.186	0.468 x 0.468 x 0.172	0.302 x 0.173 x 0.130
Space group	<i>P</i> 2 ₁ /c	<i>P</i> 2 ₁	<i>P</i> 2 ₁
<i>a</i> (Å)	11.9110(2)	9.1990(6)	9.2272(4)
<i>b</i> (Å)	12.7103(2)	10.1509(6)	10.2167(5)
<i>c</i> (Å)	15.0672(2)	13.4605(8)	13.4242(6)
β (°)	105.4247(9)	105.6051(10)	106.7643(7)
<i>V</i> (Å ³)	2198.90(6)	1210.58(13)	1211.73(10)
<i>Z</i>	4	2	2
ρ _{calc.} (g·cm ⁻³)	1.433	1.379	1.377
μ (mm ⁻¹)	12.132	1.394	1.393
F(000)	976.0	520	520
θ range for data collection (°)	3.850 to 71.891°	2.299 to 27.441	1.584 to 27.503°.
No. of reflections	28583	21402	19185
No. of independent reflections (R _{int})	4229 (0.0351)	5518 (0.0275)	5559 (0.0164)
No. of data/restr./param.	4229 / 1348 / 486	5518 / 1308 / 480	5559 / 122 / 277
Goodnes-on-fit (GOF) on F ²	1.339	1.030	1.071
R ₁ , ^a wR ₂ ^b (<i>I</i> > 2σ(<i>I</i>))	0.0508, 0.1106	0.0254, 0.0616	0.0249, 0.0632
R ₁ , ^a wR ₂ ^b (all data)	0.0511, 0.1108	0.0263, 0.0623	0.0251, 0.0634
Flack parameter	—	-0.005(7)	-0.016(17)
Largest diff. peak/hole (e·Å ⁻³)	0.879 / -0.693	0.599 / -0.610	0.406 / -0.304
CCDC	1917027	1917028	1917029

^a R₁ = $\sum ||F_o| - |F_c|| / \sum |F_o|$. ^b wR₂ = $[\sum w(F_o^2 - F_c^2)^2 / \sum (F_o^2)^2]^{1/2}$.

Single crystal X-ray diffraction details

Single crystals of all compounds were mounted on nylon loop and placed in the cold nitrogen stream (100 K) inside a Bruker APEX DUO diffractometer equipped with an Apex II CCD detector using MoK_α (λ = 0.71073 Å, (*R*)- and (*Rac*)-**13**) and CuK_α (λ = 1.54178 Å, **12**) Incoatec I_μS microsources and multilayer optic monochromators. Frames were collected using omega scans and integrated with SAINT.⁸ Multi-scan absorption correction (SADABS) was applied.⁸ The structures were solved by dual-space methods (SHELXT)⁹ and refined using full-matrix least-squares on F² with SHELXL¹⁰ within the ShelXle GUI.¹¹ Weighted R factors, wR, and all goodness-of-

fit indicators are based on F^2 . All non-hydrogen atoms were refined anisotropically. The hydrogen atoms of the C–H bonds were placed in idealized positions, whereas the hydrogen atoms from the OH moieties were localized from the difference electron density map and their positions were refined with U_{iso} tied to the parent atom with distance restraint (DFIX). The disordered groups and solvent molecules were refined using geometry (SAME/SADI and DFIX) and U_{ij} restraints (SIMU, RIGU and EADP) implemented in SHELXL.¹⁰ The molecular graphics were prepared using GRETEP, POV-RAY, and GIMP.¹²⁻¹⁴

References

- ¹ S. Liu, N. Suematsu, K. Maruoka and S. Shirakawa, *Green Chem.*, 2016, **18**, 4611–4615.
- ² Y. Toda, Y. Komiyama, A. Kikuchi and H. Suga, *ACS Catal.*, 2016, **6**, 6906–6910.
- ³ X. Meng, H. He, Y. Nie, X. Zhang, S. Zhang and J. Wang, *ACS Sustainable Chem. Eng.*, 2017, **5**, 3081–3086.
- ⁴ J. A. Castro-Osma, J. Martínez, F. de la Cruz-Martínez, M. P. Caballero, J. Fernández-Baeza, J. Rodríguez-López, A. Otero, A. Lara-Sánchez and J. Tejeda, *Catal. Sci. Technol.*, 2018, **8**, 1981–1987.
- ⁵ M. Cokoja, M. E. Wilhelm, M. H. Anthofer, W. A. Herrmann and F. E. Kühn, *ChemSusChem*, 2015, **8**, 2436–2454.
- ⁶ A. M. Hardman-Baldwin and A. E. Mattson, *ChemSusChem*, 2014, **7**, 3275–3278.
- ⁷ M. de J. Velásquez-Hernández, A. Torres-Huerta, U. Hernández-Balderas, D. Martínez-Otero, A. Núñez-Pineda and V. Jancik, *Polyhedron*, 2017, **122**, 161–171.
- ⁸ SAINT and SADABS; Bruker AXS Inc.: Madison, WI, 2007.
- ⁹ G. M. Sheldrick, SHELXT—Integrated space-group and crystal-structure determination. *Acta Crystallogr. Sect. A: Found. Adv.*, 2015, **71**, 3–8.
- ¹⁰ G. M. Sheldrick, A Short History of SHELX. *Acta Crystallogr., Sect. C: Struct. Chem.*, 2015, **71**, 3–8.
- ¹¹ C. B. Hübschle, G. M. Sheldrick and B. Dittrich, ShelXle: a Qt Graphical User Interface for SHELXL. *J. Appl. Crystallogr.*, 2011, **44**, 1281–1284.
- ¹² J. Laugier and B. Bochu, LMGP-Suite Suite of Programs for the interpretation of X-ray Experiments, ENSP/Laboratoire des Matériaux et du Génie Physique, BP 46. 38042 Saint Martin d'Hères, France. <http://www.inpg.fr/LMGP> and <http://www.ccp14.ac.uk/tutorial/lmpg/>
- ¹³ Persistence of Vision Raytracer (Version 3.6), Persistence of Vision Pty. Ltd. 2004, <http://www.povray.org>
- ¹⁴ GIMP 2.8: The GNU Image Manipulation Program. <http://www.gimp.org>.